Breathing pulses in singularly perturbed reaction-diffusion systems

Frits Veerman

Mathematical Institute, University of Oxford,
Radcliffe Observatory Quarter, Woodstock Road,
Oxford OX2 6GG, United Kingdom

15th October 2014

Abstract

The weakly nonlinear stability of pulses in general singularly perturbed reaction-diffusion systems near a Hopf bifurcation is determined using a centre manifold expansion. A general framework to obtain leading order expressions for the (Hopf) centre manifold expansion for scale separated, localised structures is presented. Using the scale separated structure of the underlying pulse, directly calculable expressions for the Hopf normal form coefficients are obtained in terms of solutions to classical Sturm-Liouville problems. The developed theory is used to establish the existence of breathing pulses in a slowly nonlinear Gierer-Meinhardt system, and is confirmed by direct numerical simulation.

1 Introduction

The study of localised patterns in systems of reaction-diffusion equations has been a very active field of research for the last couple of decades. In canonical model systems such as the Gray-Scott [17] or Gierer-Meinhardt [15] model, far-from-equilibrium patterns were constructed and analysed in the presence of an asymptotically small parameter, giving the system under consideration a singularly perturbed nature [8, 21]. This singularly perturbed structure induces a spatial scale separation, which can be used to obtain explicit leading order expressions for the pattern under consideration (e.g. [6]). These techniques were applied in full generality in [11] in the context of single pulse patterns, going beyond the existing analysis in the context of the canonical Gray-Scott and Gierer-Meinhardt models. In [32], this extended theory was applied in the context of an explicit model, exhibiting new, previously unobserved behaviour: numerical simulations revealed the existence of stable, temporally oscillating pulses.
The stability analysis of these pulse solutions in [11] led to observation that the most general pulse destabilisation scenario corresponds to a Hopf bifurcation, an observation that is also known from the extensive literature on Gray-Scott/Gierer-Meinhardt models [5, 6, 7, 10, 21, 22, 25, 29, 34]. This Hopf bifurcation, and in particular its unfolding, is the main topic of the current paper. The aim of this paper is to develop a mechanism for the weakly nonlinear analysis of the aforementioned Hopf destabilisation scenario, through local analysis of the associated centre manifold.

These 'breathing' pulses, such as observed in [32], have been an object of active research in the field of lasers and optical media during the last two decades. More generally, localised structures similar to those analysed in [11] are widely studied as optical phenomena, often in the context of the complex Ginzburg-Landau equation. Breathing localised pulses, also known as

oscillons, are frequently observed and studied both numerically and analytically, see e.g. [27]. Oscillons are considered as excitable localised structures [16, 33]. As in the context of [11], a Hopf bifurcation is often regarded as the birthplace of oscillons [12]. For a good overview of the literature on breathing pulses in optical media, see the introduction in [18]. The terminology 'breather' is also used for (sideways) oscillating fronts, often within the context of neural networks [4, 14]. See in particular [13], where a the nonlinear stability of a Hopf bifurcation in an explicit neural network system was carried out using multiple scale expansions.
In a recent publication [19], a somewhat similar approach was taken to numerically investigate breathing and moving pulses in an explicit three-dimensional reaction-diffusion system. The same system was analysed in detail in [31, 30], using similar techniques as in [11]. Therefore, the partial results in [19] can be analytically verified and extended using the analysis in the present paper on the results found in [31, 30].

The article is structured as follows. In section 2, relevant results from [11] on the existence and stability of pulse solutions are summarised, (re)introducing notation which will be used throughout the text. In section 3, the Hopf centre manifold is introduced, together with a scale separated inner product. Also, the issue of the translational eigenmode is addressed. Since the systems of reaction-diffusion equations studied in the field of pattern formation – and in extension localised pattern solutions thereof – exhibit translational invariance, the translational eigenmode with corresponding (central) eigenvalue $\lambda = 0$ is always present when the stability of the pattern under consideration is assessed. However, it turns out that the Hopf centre manifold can be foliated along the direction spanned by the translational mode (Theorem 3.3); moreover, the dynamics along the translational direction turn out to be trivial.

Section 4 is dedicated to the explicit local expansion of the centre manifold established in section 3, following the method presented in [20]. This introduces a number of new inverse problems to be solved, along with the analysis of the adjoint linear operator associated to the linearisation of the pulse solution. In order to obtain explicit expressions for the coefficients in the Hopf normal form associated with the Hopf centre manifold expansion, both the new inverse problems and the adjoint operator are treated in more detail in section 5. Here, the scale separated structure of the underlying pulse solution plays an important role. A general approach to obtain leading order expressions for the previously encountered inverse problems is presented, and it is shown how this analysis applies to the inverse problems at hand. Lastly, the scale separated inner product is used to obtain directly calculable leading order expressions for the coefficients in the Hopf normal form associated with the Hopf centre manifold expansion using leading order expressions for the pulse and its eigenmodes. Given the intricate nature of the problem, this result is quite remarkable: the formal centre manifold expansion leads to concrete, explicitly computable results, based on explicit leading order expressions for the Hopf eigenfunctions; see Corollary 5.9.

In section 6, the conditions for the existence and stability of breathing pulses are summarised in Theorem 6.1. The developed theory is then applied to a model example, the slowly nonlinear Gierer-Meinhardt equation (6.3), which was the subject of analysis in [32]. The explicit leading order expressions available for the pulse and its eigenfunctions allow one to obtain directly computable eigenvalues, and in extension directly computable values of the Hopf normal form coefficients. For this example, it is shown that the extension of the canonical Gierer-Meinhardt model with a slowly nonlinear term introduces a Hopf bifurcation which can change its nature from sub- to supercritical, depending on the parameter values (Theorem 6.2). As an aside, a relatively old observation from the literature, based on numerical simulations, is confirmed analytically [8, 34], namely that Hopf bifurcation associated with the pulse in the canonical Gierer-Meinhardt equation is always subcritical (Corollary 6.3). To the author's knowledge, this is the first time that such a numerical result is verified analytically, in a systematic fashion.

Moreover, the technical approach advocated in this paper, preferably combined with the use of symbolic algebra software such as Mathematica [2], brings the weakly nonlinear analysis of localised structures in reaction-diffusion systems within reach.

2 Preliminaries and prerequisites

In [11], a general theory for establishing the existence and stability of stationary single pulses was presented in a general setting of a singularly perturbed, two component system of reaction-diffusion equations on the real line, with asymptotically small parameter $0 < \varepsilon \ll 1$. It was shown that the most general context in which these pulse solutions could be constructed led to the following system:

$$\left\{ \begin{array}{rcrcrcr} U_t & = & U_{xx} & - & (\mu\, U - \nu_1 F_1(U;\varepsilon)) & + & \frac{\nu_2}{\varepsilon} F_2(U,V;\varepsilon) \\ V_t & = & \varepsilon^2 V_{xx} & - & V & + & G(U,V;\varepsilon) \end{array} \right. . \tag{2.1}$$

System (2.1) is considered on the unbounded domain such that $U, V : \mathbb{R} \times \mathbb{R}_{>0} \to \mathbb{R}$; moreover, we restrict ourselves to positive solutions. A stable homogeneous trivial background state is assumed. The range of the model parameters $\mu, \nu_{1,2}$ and mild regularity assumptions on the nonlinear reaction terms $F_{1,2}$ and G are specified in (A1 - A4) of (upcoming) Assumptions 2.2. In the following subsections 2.1 and 2.2, a very concise overview of the results obtained in [11] is given. The necessary ingredients for establishing localised pulses and their eigenfunctions are presented, in order to be able to set up the theory for a Hopf bifurcation of such a localised pulse, which is the main subject of this paper. By nature, this overview is far from complete and very brief: the reader is encouraged to consider [11] for a complete exposition.

2.1 Existence result on pulse solutions

The purpose of this subsection is to introduce the ingredients which are necessary to formulate Result 2.3 for the existence of pulse solutions to (2.1). We refer the reader to [11] for the full geometric analysis and corresponding Theorem 2.1 therein.

Introducing the 'fast' (or short scale) coordinate $\xi = \frac{x}{\varepsilon}$, (2.1) can be transformed into

$$\left\{ \begin{array}{rcrcrcr} U_t & = & \frac{1}{\varepsilon^2} U_{\xi\xi} & - & (\mu\, U - \nu_1 F_1(U;\varepsilon)) & + & \frac{\nu_2}{\varepsilon} F_2(U,V;\varepsilon) \\ V_t & = & V_{\xi\xi} & - & V & + & G(U,V;\varepsilon) \end{array} \right. . \tag{2.2}$$

Establishing the existence of a stationary pulse solution to (2.2) (or equivalently (2.1)) which is asymptotic to the (stable) trivial background state of (2.2) is equivalent to constructing a homoclinic orbit in the associated ODE system

$$\left\{ \begin{array}{rcl} u_\xi & = & \sqrt{\varepsilon} p \\ p_\xi & = & \sqrt{\varepsilon}\,(-\nu_2 F_2(u,v;\varepsilon) + \varepsilon\,(\mu u - \nu_1 F_1(u;\varepsilon))) \\ v_\xi & = & q \\ q_\xi & = & v - G(u,v;\varepsilon) \end{array} \right. . \tag{2.3}$$

The slow-fast structure present in the ODE system (2.3) leads to a scale separation between the U- and V-components of the pulse. One can within the unbounded domain define an inner, 'fast' region

$$I_f = \left[-\frac{1}{\varepsilon^{\frac{1}{4}}}, \frac{1}{\varepsilon^{\frac{1}{4}}} \right], \tag{2.4}$$

where the U-component of the pulse will be constant to leading order in ε, while outside I_f the V-component of the pulse will be exponentially small; see Figure 1 and Result 2.3.

In order to formulate the existence result, we introduce the fast reduced system

$$v_{f,\xi\xi} = v_f - G(u_0, v_f; 0) \text{ or } \left\{ \begin{array}{rcl} v_{f,\xi} &=& q_f \\ q_{f,\xi} &=& v_f - G(u_0, v_f; 0) \end{array} \right. , \ u_0 > 0 \text{ constant}, \tag{2.5}$$

and the slow reduced system

$$u_{s,xx} = \mu u_s - \nu_1 F_1(u_s; \varepsilon), \text{ or } \left\{ \begin{array}{rcl} u_{s,x} &=& p_s \\ p_{s,x} &=& \mu u_s - \nu_1 F_1(u_s; \varepsilon) \end{array} \right. , \ u > 0. \tag{2.6}$$

Moreover, we define

$$D_p(u_0) = \int_{-\infty}^{\infty} F_2(u_0, v_{f,h}(\xi; u_0); 0)\, \mathrm{d}\xi, \tag{2.7}$$

to formulate the 'existence criterion'

$$\mu u^2 - 2\nu_1 \int_0^u F_1(\tilde{u}; 0)\, d\tilde{u} = \tfrac{1}{4}\nu_2^2\, D_p^2(u) = \tfrac{1}{4}\nu_2^2 \left[\int_{-\infty}^{\infty} F_2(u, v_{f,h}(\xi; u); 0)\, \mathrm{d}\xi \right]^2. \tag{2.8}$$

In [11], it was shown that for each solution u_* to (2.8) there exists a symmetric, stationary pulse solution to (2.1)/(2.2).

We now state the assumptions on the model functions $F_{1,2}$ and G, the model parameters $\mu, \nu_{1,2}$, the fast system (2.5) and the function $D_p(u)$ (2.7); for the reasoning behind these assumptions, see [11]. Note that the Gray-Scott and Gierer-Meinhardt models are important, canonical examples of systems obeying these assumptions; however, the full class of systems described in this way is far more encompassing.

Definition 2.1. *A statement of the form '$f(x) \rightsquigarrow c \cdot g(x)$ as $x \to x_0$' is true whenever the limit $\lim_{x\to x_0} \frac{1}{g(x)} f(x) = c$ exists and is well-defined.*

Assumptions 2.2. *The following is assumed to hold:*

(A1) *μ, $\nu_{1,2}$ are real and nonsingular in ε; furthermore, $\mu > 0$.*

(A2) *$F_1(U; \varepsilon) \rightsquigarrow U^{f_1}$ as $U \downarrow 0$ for some $f_1 > 1$;*
F_1 is smooth both on its domain and as a function of ε.

(A3) *Writing $F_2(U, V; \varepsilon) = F_{2,1}(U; \varepsilon)\, V + F_{2,2}(U, V; \varepsilon)$,*
$F_{2,1}(U; \varepsilon) \rightsquigarrow \tilde{F}_{2,1}(\varepsilon)\, U^{\gamma_1}$ as $U \downarrow 0$ for some $\gamma_1 \geq 0$ and $\tilde{F}_{2,1}(\varepsilon) \in \mathbb{R}$;
$F_{2,2}(U, V; \varepsilon) \rightsquigarrow \tilde{F}_{2,2,u}(V; \varepsilon)\, U^{\alpha_1}$ as $U \downarrow 0$ for some $\alpha_1 \in \mathbb{R}$;
$F_{2,2}(U, V; \varepsilon) \rightsquigarrow \tilde{F}_{2,2,v}(U; \varepsilon)\, V^{\beta_1}$ as $V \to 0$ for some $\beta_1 > 1$;
F_2 is smooth both on its domain and as a function of ε.

(A4) *$G(U, V; \varepsilon) \rightsquigarrow \tilde{G}_u(V; \varepsilon)\, U^{\alpha_2}$ as $U \downarrow 0$ for some $\alpha_2 \in \mathbb{R}$;*
$G(U, V; \varepsilon) \rightsquigarrow \tilde{G}_v(U; \varepsilon)\, V^{\beta_2}$ as $V \to 0$ for some $\beta_2 > 1$;
G is smooth both on its domain and as a function of ε.

(A5) *For all $u_0 > 0$ there exists a positive solution $v_{f,h}(\xi; u_0)$ to (2.5) which is homoclinic to $(v_f, q_f) = (0, 0)$.*

(A6) *$D_p(u) \rightsquigarrow 1 \cdot u^{d_p}$ as $u \downarrow 0$ for some $d_p \in \mathbb{R}$, c.f. (2.7).*

The following Existence Result is a summary of Theorem 2.1 in [11]; see Figure 1 for an illustration.

Result 2.3 (Existence and structure of pulse solutions). *Assume that conditions 2.2 hold and let $\varepsilon > 0$ be small enough. Let u_* be a non-degenerate solution to (2.8). Then (2.2) admits a stationary pulse solution $\Gamma_h(\xi) = (U_h(\xi), V_h(\xi))^T$ which is symmetric in $\xi = 0$. Furthermore, there are $O(1)$ constants $C_{1,2} > 0$ such that the following holds:*

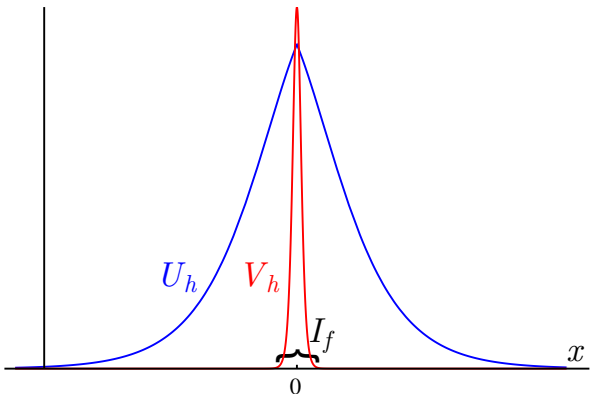

Figure 1: A sketch of the stationary, symmetric pulse solution to (2.2), whose existence and structure follows from Result 2.3. For clarity of presentation, the slow variable $x = \varepsilon\xi$ (instead of the fast variable ξ) is plotted on the horizontal axis.

- $\Gamma_h(\xi) = \begin{pmatrix} u_{s,0}(x_* + \varepsilon\xi) \\ 0 \end{pmatrix} + C_1 e^{-C_2\xi}$ *for* $\xi > \varepsilon^{-\frac{1}{4}}$;
- $\Gamma_h(\xi) = \begin{pmatrix} u_{s,0}(x_* - \varepsilon\xi) \\ 0 \end{pmatrix} + C_1 e^{C_2\xi}$ *for* $\xi < -\varepsilon^{-\frac{1}{4}}$;
- $\Gamma_h(\xi) = \begin{pmatrix} u_* \\ v_{f,h}(\xi; u_*) \end{pmatrix} + O(\varepsilon^{\frac{3}{4}})$ *for* $\xi \in I_f$.

Here, $v_{f,h}(\xi; u_*)$ is the homoclinic solution to (2.5) *introduced in Assumptions 2.2, (A5); $u_{s,0}$ is the (unique) solution to* (2.6) *which is forward asymptotic to the origin, i.e.* $\lim_{x\to\infty} u_{s,0}(x) = 0$. *The coordinate x_* is such that $u_{s,0}(x_*) = u_*$.*

2.2 Pulse stability, linearisation and eigenfunctions

In order to set up an analysis of Hopf bifurcations of the localised pulses considered in the previous section, it is necessary to highlight some aspects of the stability analysis of such a pulse, as carried out in [11], section 3. The main purpose of this subsection is to give a leading order expression for the eigenfunctions associated to the stability problem of such a localised pulse, summarised in Result 2.4. The exposition presented in this subsection is (again) very brief. The full and detailed analysis can be found in [11], section 3.

In the following, assume that Result 2.3 holds. The stability analysis of the resulting pulse Γ_h is closely related to the study of the linear operator

$$\mathcal{L}(\xi;\varepsilon) = \begin{pmatrix} \varepsilon^{-2} & 0 \\ 0 & 1 \end{pmatrix} \frac{\mathrm{d}^2}{\mathrm{d}\xi^2} - \mathcal{A}(\xi;\varepsilon), \tag{2.9}$$

where

$$\mathcal{A}(\xi;\varepsilon) = \left.\begin{pmatrix} \mu - \nu_1 \frac{\mathrm{d}F_1}{\mathrm{d}U} - \frac{\nu_2}{\varepsilon}\frac{\partial F_2}{\partial U} & -\frac{\nu_2}{\varepsilon}\frac{\partial F_2}{\partial V} \\ -\frac{\partial G}{\partial U} & 1 - \frac{\partial G}{\partial V} \end{pmatrix}\right|_{(U,V)=(U_h(\xi),V_h(\xi))}. \tag{2.10}$$

Since $\lim_{\xi\to\pm\infty} \Gamma_h(\xi) = (0,0)$, the matrix $\mathcal{A}(\xi;\varepsilon)$ is asymptotically constant as $\xi \to \pm\infty$, i.e. $\lim_{\xi\to\pm\infty} \mathcal{A}(\xi;\varepsilon) = \mathcal{A}_\infty(\varepsilon)$. The eigenvalues of this constant matrix $\mathcal{A}_\infty(\varepsilon)$ determine the essential spectrum σ_e of the operator $\mathcal{L}$, which is given by

$$\sigma_e = \{\lambda \in \mathbb{R} : \lambda \leq \max(-\mu, -1)\} \subset \mathbb{C}. \tag{2.11}$$

The slow-fast structure of the pulse Γ_h, made explicit in Result 2.3, is inherited by the linear operator $\mathcal{L}$; it has the obvious interpretation of being the linearisation of (2.2) around Γ_h. One can therefore introduce the 'fast' linear operator

$$\mathcal{L}_f(\xi) = \frac{\mathrm{d}^2}{\mathrm{d}\xi^2} - \left[1 - \frac{\partial G}{\partial V}(u_*, v_{f,h}(\xi; u_*))\right], \quad \xi \in \mathbb{R}, \tag{2.12}$$

with u_* and $v_{f,h}$ as in Result 2.3, and determine its spectrum. The associated eigenvalue problem $\left(\mathcal{L}_f - \lambda\right) v = 0$ is of Sturm-Liouville type; relevant results from the literature are summarised in [11], Lemma 3.2. Based on those results, let $\lambda_{f,j}$, $j \in \mathbb{Z}_{\geq 0}$ be the eigenvalues of the linear operator $\mathcal{L}_f$ acting on the space of bounded integrable functions on the entire real line.
Similarly, the 'slow' linear operator

$$\mathcal{L}_s(x) = \frac{\mathrm{d}^2}{\mathrm{d}x^2} - \left[\mu - \nu_1 \frac{\partial F_1}{\partial U}(u_{s,0}(x_* + x))\right], \quad x \geq 0, \tag{2.13}$$

with $u_{s,0}$ as in Result 2.3, plays a central role in the spectral analysis of $\mathcal{L}$. The eigenvalue problem $(\mathcal{L}_s - \lambda)\, u = 0$ is again of Sturm-Liouville type, albeit on the positive halfline. Let $u_{s,-}(x;\lambda)$ be the solution to the eigenvalue problem $\mathcal{L}_s u = \lambda\, u$ that is bounded as $x \to \infty$, such that $u_{s,-}(x;\lambda) \rightsquigarrow 1 \cdot e^{-\sqrt{\mu+\lambda}\, x}$ as $x \to \infty$.

The coupling between the U- and V-components of the pulse (apparent in the off-diagonal entries of $\mathcal{A}$) manifests itself in the spectral analysis of $\mathcal{L}$ through the nonhomogeneous problem

$$\left(\mathcal{L}_f - \lambda\right) v = -\frac{\partial G}{\partial U}(u_*, v_{f,h}(\xi; u_*)), \quad \xi \in \mathbb{R}. \tag{2.14}$$

For $\lambda \neq \lambda_{f,j}$ and $\lambda \notin \sigma_e$, let $v_{\mathrm{in}}(\xi;\lambda)$ be the unique bounded solution to (2.14). The existence and uniqueness of v_{in} follows from the analysis in [11], section 3, which is based on the Fredholm alternative. Note that it immediately follows that v_{in} is even as a function of ξ, i.e. $v_{\mathrm{in}}(\xi;\lambda) = v_{\mathrm{in}}(-\xi;\lambda)$.

The actual spectral analysis of $\mathcal{L}$ (2.9) does not need to be summarised here: for an overview of this spectral analysis, using an Evans function approach, see [11], sections 4 and 5. There, a leading order expression for the Evans function was derived ([11], Theorem 4.4), enabling direct calculation of the pulse eigenvalues. The most relevant result for the current paper however is Corollary 5.10 therein; it was shown that the most general destabilisation scenario for a localised pulse in (2.2) is through a Hopf bifurcation. That observation will be the starting point of the analysis presented in this paper. However, some comments on the trivial eigenvalue are in order; they can be found in the next section, section 2.3.

The following Result, which summarises results from section 4 in [11], characterises the leading order behaviour of eigenfunctions of the linear operator $\mathcal{L}$ (2.9). This leading order behaviour will be very instrumental in the upcoming analysis.

Result 2.4 (**Existence and structure of eigenfunctions**). *Let $\varepsilon > 0$ be small enough. Assume that $\lambda \notin \sigma_e$ and $\lambda \neq \lambda_{f,j}$. If there is a $\lambda \in \mathbb{C}$ for which there is a bounded integrable function $\phi : \mathbb{R} \to \mathbb{C}^2$ such that $\mathcal{L}(\xi;\varepsilon)\,\phi(\xi;\lambda,\varepsilon) = \lambda\,\phi(\xi;\lambda,\varepsilon)$, then $\phi(\xi;\lambda,\varepsilon)$ is unique. Furthermore, there are $O(1)$ constants $C_{1,2}$ such that the following holds:*

- $\phi(\xi;\lambda,\varepsilon) = \begin{pmatrix} u_{s,-}(\varepsilon\xi;\lambda) \\ 0 \end{pmatrix} + C_1 e^{-|C_2|\xi}$ *for* $\xi > \varepsilon^{-\frac{1}{4}}$;
- $\phi(\xi;\lambda,\varepsilon) = \phi(-\xi;\lambda,\varepsilon)$ *for* $\xi < -\varepsilon^{-\frac{1}{4}}$;

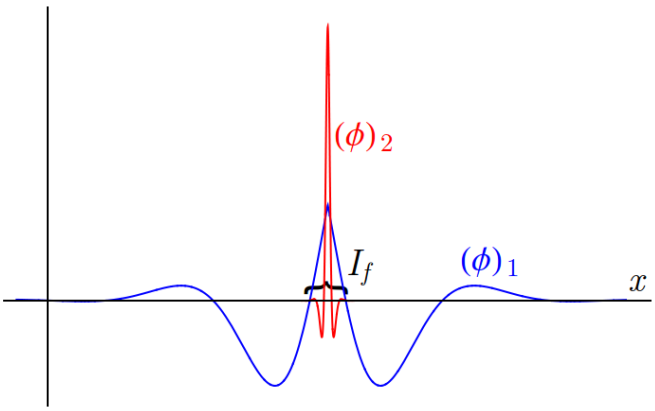

Figure 2: A sketch of a possible eigenfunction ϕ of $\mathcal{L}(\xi, \varepsilon)$ (2.9) whose structure is described in Result 2.4. Note that the eigenfunction inherits the scale separated structure from the stationary pulse, c.f. Figure 1. The first (slow) resp. second (fast) component of the eigenfunction ϕ are indicated by $(\phi)_1$ resp. $(\phi)_2$. For clarity of presentation, the slow variable $x = \varepsilon\xi$ (instead of the fast variable ξ) is plotted on the horizontal axis.

- $\phi(\xi; \lambda, \varepsilon) = u_{s,-}(0; \lambda)\begin{pmatrix} 1 \\ v_{\text{in}}(\xi; \lambda) \end{pmatrix} + O(\varepsilon^{\frac{3}{4}})$ *for* $\xi \in I_f$.

The leading order expressions for the eigenfunction of $\mathcal{L}$ are based on the proof of Theorem 4.4 in [11].

2.3 Translational symmetry and the trivial eigenvalue

This subsection focuses on the well-known fact that the trivial eigenvalue $\lambda = 0$ is always part of the spectrum of a localised structure. This has some implications for the centre manifold analysis in the upcoming section 3. To treat and separate the contribution of the trivial eigenmode to the centre manifold in a systematic fashion, some concepts and symbols are introduced the current subsection, for later use.

A general n-component reaction-diffusion equation

$$\tilde{u}_t = D\tilde{u}_{xx} + f(\tilde{u}), \quad \tilde{u} \in \mathbb{R}^n, \ D \in \text{Mat}(n, \mathbb{R}), \ f : \mathbb{R}^n \to \mathbb{R}^n \tag{2.15}$$

is equivariant under the continuous one-parameter group of isometries $(T_\alpha)_{\alpha\in\mathbb{R}}$ which acts as

$$T_\alpha\tilde{u}(x) = \tilde{u}(x + \alpha). \tag{2.16}$$

Every stationary solution $\tilde{u}_0$ to (2.15), for which

$$D\tilde{u}_{0,xx} + f(\tilde{u}_0) = 0, \tag{2.17}$$

can therefore be thought of as representing a continuous family of stationary solutions $(T_\alpha\tilde{u}_0)_{\alpha\in\mathbb{R}}$, obtained under the group action T_α. Since the infinitesimal generator of this underlying translational symmetry group (2.16) is $\tau = \frac{\partial}{\partial x}$, it follows from (2.17) that $\tau\tilde{u}_0 = \tilde{u}_{0,x}$ obeys the linear equation

$$\left[D\frac{\partial^2}{\partial x^2} + \frac{\mathrm{d}f}{\mathrm{d}\tilde{u}}(\tilde{u}_0)\right]\tau\tilde{u}_0 = 0. \tag{2.18}$$

The above considerations apply to the PDE system (2.1)/(2.2); in particular, for the homoclinic pulse solution whose existence was established in Result 2.3. In this context, (2.18) takes the form

$$\mathcal{L}\frac{\mathrm{d}}{\mathrm{d}\xi}\Gamma_h = 0,$$

from which follows that $\lambda = 0$ is always an eigenvalue of the operator $\mathcal{L}$ (2.9), with eigenfunction $\frac{\mathrm{d}}{\mathrm{d}\xi}\Gamma_h$. Note that Result 2.4 does not apply for this eigenvalue, since $\lambda_{f,1} = 0$. The fact that indeed $\lambda_{f,1} = 0$ can be found in [11]; also, the above argument can be applied to (2.5) with its linearisation (2.12) around the orbit $v_{f,h}$, Assumptions 2.2 (A5). However, the eigenfunction $\frac{\mathrm{d}}{\mathrm{d}\xi}\Gamma_h$ does exhibit the same scale separated structure as the eigenfunctions described in Result 2.4, see Result 2.3 for the structure of Γ_h. Both considerations will be of importance in the next section, where a centre manifold analysis will be set up.

3 The Hopf centre manifold

In this paper, we focus on the situation where the pulse Γ_h undergoes a Hopf bifurcation. In other words, let $(\mu, \nu_1, \nu_2) = (\mu_H, \nu_{1,H}, \nu_{2,H})$ be such that there is a bounded integrable function $\phi_H : \mathbb{R} \to \mathbb{C}^2$ as in Result 2.4 for which

$$\mathcal{L}\phi_H = i\,\omega_H\phi_H, \tag{3.1}$$

with $\omega_H > 0$. Since the operator $\mathcal{L}$ is real, it immediately follows that the Hopf bifurcation (3.1) yields a complex conjugate pair of eigenvalues $\pm i\,\omega_H$ with associated eigenfunction pair $\left\{\phi_H, \overline{\phi_H}\right\}$ – here and henceforth, complex conjugation will be denoted by an overline.

Since the linear operator $\mathcal{L}$ (2.9) is sectorial and its continuous spectrum is completely determined by the essential spectrum σ_e (2.11), we can infer that its central spectrum

$$\sigma_0 = \{\lambda \in \mathbb{C} : \lambda \text{ is in the spectrum of } \mathcal{L},\ \mathrm{Re}(\lambda) = 0\}$$

consists of finitely many eigenvalues. Moreover, $\lambda = 0 \in \sigma_0$ (see subsection 2.3); we assume that this trivial eigenvalue is nondegenerate. As mentioned before, it was argued in [11] that this is the most general destabilisation scenario for a given pulse whose existence is ensured by Result 2.3. Indeed, this destabilisation through a Hopf bifurcation is typical for pulses in both the Gierer-Meinhardt equation [6] and its slowly nonlinear counterpart, see [32], sections 4 and 5.
Henceforth, we assume $\pm i\,\omega_H$ are the only nontrivial central eigenvalues, i.e. that the central spectrum of $\mathcal{L}$ is given by

$$\sigma_{0,H} = \{\pm i\,\omega_H, 0\}\,. \tag{3.2}$$

Moreover, based our insight in the general pulse destabilisation mechanisms from [11], we assume that the Hopf bifurcation under consideration is of codimension 1, such that the Hopf eigenvalues are simple.

To carry out a centre manifold analysis for this central spectrum, one would naively aim for an expansion in the three associated eigenvectors. However, the translational symmetry (2.16) of (2.1)/(2.2), being the source of the trivial central eigenvalue $\lambda = 0$, induces a transversal structure for the centre manifold, enabling one to effectively ignore the translational eigenmode in the local centre manifold expansion (see upcoming Theorem 3.3). To set the stage, we first focus on the ambient function space where the centre manifold will be embedded in.

3.1 Choosing a function space

In order to properly set up the centre manifold theory for the pulse Γ_h at the Hopf bifurcation (3.1), we need choose an appropriate function space to work in. To accommodate for the fact that we want to make use of the leading order expressions of the constituents, like ϕ_H, which will have a scale separated structure, we search for an inner product which behaves 'nicely' under the limit $\varepsilon \downarrow 0$. To that end, we introduce the function space

$$\mathcal{X} = L_2(\mathbb{R}, \mathbb{C}^2; \mu_\varepsilon) \tag{3.3}$$

with the partly scaled Lebesgue measure μ_ε defined such that the associated inner product $\langle \cdot, \cdot \rangle$ can be defined as

$$\langle \phi, \psi \rangle = \int_{\mathbb{R}} \phi^T S \, \overline{\psi} \, \mathrm{d}\xi \quad \text{with} \quad S = \begin{pmatrix} \varepsilon & 0 \\ 0 & 1 \end{pmatrix} \tag{3.4}$$

for $\phi, \psi \in \mathcal{X}$. In other words: the product of the first components is integrated over the large scale variable $x = \varepsilon\xi$, the product of the second components over the small scale variable ξ. Note that the norm induced by the inner product (3.4) is for all $\varepsilon > 0$ equivalent to the 'standard' norm on $(L_2(\mathbb{R}, \mathbb{C}))^2$, making $\mathcal{X}$ and $(L_2(\mathbb{R}, \mathbb{C}))^2$ isometrically isomorphic as metric spaces. A similar norm was introduced in [9].

3.2 Foliation of the centre manifold along the translational eigenmode

In this section, we show that the influence of the translational eigenmode can be separated completely from the other eigendirections. We follow the general approach in [20], section 2.3.3 therein. A similar treatment can be found in [23], which is partly based on the general theory developed in [24]. The choice to follow [20] in the current paper is solely for notational purposes.

To make full use of the translational symmetry of (2.2), we choose local tubular coordinates to separate the perturbation of the stationary pulse solution Γ_h into a perturbation along resp. perpendicular to the orbits of the translation group $(T_\alpha)_{\alpha \in \mathbb{R}}$, as follows:

$$\begin{pmatrix} U(\xi, t) \\ V(\xi, t) \end{pmatrix} = \Gamma(\xi, t) = T_{\alpha(t)} \left(\Gamma_h(\xi) + \rho(\xi, t) \right), \tag{3.5}$$

where

$$\langle \rho, \frac{\mathrm{d}}{\mathrm{d}\xi} \Gamma_h \rangle = 0. \tag{3.6}$$

In the tubular coordinates (3.5), the left-hand side of (2.2) yields

$$\begin{pmatrix} U_t \\ V_t \end{pmatrix} = \frac{\partial}{\partial t} \Gamma = \frac{\mathrm{d}\alpha}{\mathrm{d}t} \, T_{\alpha(t)} \left(\frac{\mathrm{d}}{\mathrm{d}\xi} \Gamma_h(\xi) + \frac{\partial}{\partial \xi} \rho(\xi, t) \right) + T_{\alpha(t)} \frac{\partial}{\partial t} \rho(\xi, t); \tag{3.7}$$

(left) multiplication with $T_{-\alpha(t)}$ gives

$$T_{-\alpha(t)} \begin{pmatrix} U_t \\ V_t \end{pmatrix} = \frac{\mathrm{d}\alpha}{\mathrm{d}t} \left(\frac{\mathrm{d}}{\mathrm{d}\xi} \Gamma_h(\xi) + \frac{\partial}{\partial \xi} \rho(\xi, t) \right) + \frac{\partial}{\partial t} \rho(\xi, t). \tag{3.8}$$

Since the right-hand side of (2.2) is equivariant under the translation $T_{\alpha(t)}$, using the tubular coordinates (3.5) in the right-hand side of (2.2) and subsequent (left) multiplication with the inverse translation $T_{-\alpha(t)}$ is equivalent to substitution of $\Gamma_h(\xi) + \rho(\xi, t)$:

$$T_{-\alpha(t)} \begin{pmatrix} U_t \\ V_t \end{pmatrix} = \mathrm{RHS}(\Gamma_h(\xi) + \rho(\xi, t)) \tag{3.9}$$

with

$$\mathrm{RHS}\left((U,V)^T\right) = \begin{pmatrix} \frac{1}{\varepsilon^2}U_{\xi\xi} & - & (\mu\, U - \nu_1 F_1(U;\varepsilon)) & + & \frac{\nu_2}{\varepsilon}F_2(U,V;\varepsilon) \\ V_{\xi\xi} & - & V & + & G(U,V;\varepsilon) \end{pmatrix}. \tag{3.10}$$

Based on the orthogonality condition (3.6), we can project both sides of (3.9) onto the subspace spanned by $\frac{\mathrm{d}}{\mathrm{d}\xi}\Gamma_h$ to obtain separate dynamical equations for $\frac{\mathrm{d}\alpha}{\mathrm{d}t}$ and $\frac{\partial}{\partial t}\rho(\xi,t)$, using (3.8). Introducing the projection

$$\Pi_0 = \frac{\langle \cdot, \frac{\mathrm{d}}{\mathrm{d}\xi}\Gamma_h\rangle}{\langle \frac{\mathrm{d}}{\mathrm{d}\xi}\Gamma_h, \frac{\mathrm{d}}{\mathrm{d}\xi}\Gamma_h\rangle}\,\frac{\mathrm{d}}{\mathrm{d}\xi}\Gamma_h, \tag{3.11}$$

we see that projecting (3.8) onto the subspace spanned by $\frac{\mathrm{d}}{\mathrm{d}\xi}\Gamma_h$ yields

$$\Pi_0\, T_{-\alpha(t)}\begin{pmatrix} U_t \\ V_t \end{pmatrix} = \frac{\mathrm{d}\alpha}{\mathrm{d}t}\left(1 + \frac{\langle \frac{\partial}{\partial\xi}\rho, \frac{\mathrm{d}}{\mathrm{d}\xi}\Gamma_h\rangle}{\langle \frac{\mathrm{d}}{\mathrm{d}\xi}\Gamma_h, \frac{\mathrm{d}}{\mathrm{d}\xi}\Gamma_h\rangle}\right)\frac{\mathrm{d}}{\mathrm{d}\xi}\Gamma_h. \tag{3.12}$$

Combining this with the projection of (3.9) onto the same subspace, we can express $\frac{\mathrm{d}\alpha}{\mathrm{d}t}$ as

$$\frac{\mathrm{d}\alpha}{\mathrm{d}t} = \frac{\langle \mathrm{RHS}(\Gamma_h(\xi)+\rho(\xi,t)), \frac{\mathrm{d}}{\mathrm{d}\xi}\Gamma_h\rangle}{\langle \frac{\mathrm{d}}{\mathrm{d}\xi}\Gamma_h, \frac{\mathrm{d}}{\mathrm{d}\xi}\Gamma_h\rangle + \langle \frac{\partial}{\partial\xi}\rho, \frac{\mathrm{d}}{\mathrm{d}\xi}\Gamma_h\rangle}. \tag{3.13}$$

Note that (3.13) does *not* depend explicitly on $\alpha(t)$: this is a direct consequence of the equivariance of (2.2) under the translation group $(T_\alpha)_{\alpha\in\mathbb{R}}$.
The projection onto the orthogonal complement of the subspace spanned by $\frac{\mathrm{d}}{\mathrm{d}\xi}\Gamma_h$, given by $\mathbb{I}-\Pi_0$, can be used to obtain a dynamical equation for $\rho(\xi,t)$. Applying $\mathbb{I}-\Pi_0$ on (3.9) and using (3.13) yields

$$\begin{aligned} \frac{\partial}{\partial t}\rho(\xi,t) &= (\mathbb{I}-\Pi_0)\,\mathrm{RHS}(\Gamma_h(\xi)+\rho(\xi,t)) - \frac{\mathrm{d}\alpha}{\mathrm{d}t}\,(\mathbb{I}-\Pi_0)\,\frac{\partial}{\partial\xi}\rho \\ &= \mathrm{RHS}(\Gamma_h(\xi)+\rho(\xi,t)) - \left(\frac{\mathrm{d}}{\mathrm{d}\xi}\Gamma_h + \frac{\partial}{\partial\xi}\rho\right)\frac{\langle \mathrm{RHS}(\Gamma_h(\xi)+\rho(\xi,t)), \frac{\mathrm{d}}{\mathrm{d}\xi}\Gamma_h\rangle}{\langle \frac{\mathrm{d}}{\mathrm{d}\xi}\Gamma_h + \frac{\partial}{\partial\xi}\rho, \frac{\mathrm{d}}{\mathrm{d}\xi}\Gamma_h\rangle}. \end{aligned} \tag{3.14}$$

The decoupling of the translational perturbation parametrised by $\alpha(t)$ and the 'orthogonal' perturbation $\rho(\xi,t)$ is made rigorous in the following theorem. It is an adaptation of Theorem 3.19 from chapter 2 in [20], reformulated to suit the context of this article:

Theorem 3.1 (**Centre manifolds in presence of continuous symmetry**). *Let $\mathcal{X} = \Pi_0\mathcal{X}\oplus\mathcal{X}' = \mathrm{span}\left\{\frac{\mathrm{d}}{\mathrm{d}\xi}\Gamma_h\right\}\oplus\mathcal{X}'$, $\mathcal{L}' = (\mathbb{I}-\Pi_0)\,\mathcal{L}$ and let σ_0' be the central spectrum of $\mathcal{L}'$. Assume that σ_0' is finite, and let $\mathcal{E}_0'\subset\mathcal{X}'$ be the associated spectral subspace. Let $\mathcal{U}'\subset\mathcal{X}'$ be a neighbourhood of the origin in $\mathcal{X}'$. Consider the tubular neighbourhood*

$$\mathcal{U} = \{T_\alpha(\Gamma_h+\rho);\, \rho\in\mathcal{U}',\, \alpha\in\mathbb{R}\}\subset\mathcal{X}$$

of the line of equilibria $\{T_\alpha\,\Gamma_h,\ \alpha\in\mathbb{R}\}$.
There exists a map Ψ which has the same degree of smoothness as the right-hand side of (2.2)*, $\Psi : \mathcal{E}_0'\to\mathcal{X}'-\mathcal{E}_0'$, with $\Psi(0)=0$, $D\Psi(0)=0$ such that the manifold*

$$\mathcal{M}_0 = \left\{T_\alpha\left(\Gamma_h+\rho_0+\Psi(\rho_0)\right);\, \rho_0\in\mathcal{E}_0',\, \alpha\in\mathbb{R}\right\}\subset\mathcal{X}$$

has the following properties:

1. *The manifold $\mathcal{M}_0$ is locally invariant under* (2.2)*, in other words, if $\Gamma(\xi,t) = (U(\xi,t),V(\xi,t))^T$ is a solution of* (2.2) *satisfying $\Gamma(\xi,0)\in\mathcal{M}_0\cap\mathcal{U}$ and $\Gamma(\xi,t)\in\mathcal{U}$ for all $t\in[0,T]$, then $\Gamma(\xi,t)\in\mathcal{M}_0$ for all $t\in[0,T]$.*

2. *$\mathcal{M}_0$ contains the set of solutions of* (2.2) *staying in $\mathcal{U}$ for all $t > 0$, in other words, if Γ is a solution of* (2.2) *satisfying $\Gamma(\xi, t) \in \mathcal{U}$ for all $t > 0$, then $\Gamma(\xi, 0) \in \mathcal{M}_0$.*

The solutions to (2.2) *which stay close to the line of equilibria for all $t > 0$ are of the form* (3.5)*, with $\alpha(t)$ satisfying* (3.13) *and $\rho(\xi, t)$ satisfying* (3.14)*.*

Up to this point, our analysis only used the translational equivariance of (2.2). It will become clear that the results on the (specific form of) the eigenfunctions of $\mathcal{L}$ (2.9) as stated in Result 2.4 will enable us to drastically simplify the dynamical equation for $\alpha(t)$, as given in (3.13). The following observation will be important enough in the following to state it as a Lemma:

Lemma 3.2. *Let the conditions of Result 2.4 be fulfilled, and let λ be an eigenvalue of $\mathcal{L}$ with eigenfunction $\phi(\xi; \lambda, \varepsilon)$. Then*

$$\langle \phi, \frac{\mathrm{d}}{\mathrm{d}\xi}\Gamma_h \rangle = 0. \tag{3.15}$$

Proof. Since the stationary pulse solution Γ_h is symmetric, it is even as a function of ξ, see Result 2.3. Therefore $\frac{\mathrm{d}}{\mathrm{d}\xi}\Gamma_h$ is odd as a function of ξ. Now, from the definition of $\mathcal{L}$ (2.9) it is clear that $\mathcal{L}(\xi)$ is invariant under reflection: $\mathcal{L}(-\xi) = \mathcal{L}(\xi)$. This means that, if $\phi(\xi; \lambda, \varepsilon)$ is an eigenfunction of $\mathcal{L}$ with eigenvalue λ, then $\phi(-\xi; \lambda, \varepsilon)$ must also be an eigenfunction of $\mathcal{L}$ for that same eigenvalue (note that $\lambda \neq 0$); furthermore, $\phi(-\xi; \lambda, \varepsilon)$ is also bounded. Since the eigenfunction $\phi(\xi; \lambda, \varepsilon)$ is unique (see Result 2.4), it follows that $\phi(-\xi; \lambda, \varepsilon) = \phi(\xi; \lambda, \varepsilon)$. From the observation that the product of an even function and an odd function is odd, and that the integral of an odd function vanishes identically, the statement (3.15) follows from the definition of the inner product (3.4). □

Based on the above results (which in particular hold for the nonzero eigenvalues in our codimension 1 central spectrum (3.2)), we can formulate a theorem on the local structure of the centre manifold associated to the Hopf bifurcation (3.1) and the associated central spectrum (3.2).

Theorem 3.3. *Let the central spectrum of $\mathcal{L}$ be given by* (3.2)*. The associated centre manifold $\mathcal{M}_{0,H}$ can be foliated along the line of equilibria $\{T_\alpha \Gamma_h,\ \alpha \in \mathbb{R}\}$, and has a locally trivial product structure:*

$$\mathcal{M}_{0,H} = \mathbb{R} \times \mathcal{M}'_{0,H}.$$

The dynamics along the translational direction are trivial: equation (3.13) *simplifies to $\frac{\mathrm{d}\alpha}{\mathrm{d}t} = 0$. The full dynamics on $\mathcal{M}_{0,H}$ can be represented by the reduced dynamics on $\mathcal{M}'_{0,H}$, given by*

$$\frac{\partial}{\partial t}\rho(\xi, t) = \mathrm{RHS}(\Gamma_h(\xi) + \rho(\xi, t)). \tag{3.16}$$

Theorem 3.3 on the foliation of a Hopf centre manifold along the direction spanned by the translational eigenmode is a quite well-known result; it was proven in [23] for front solutions (see Theorem 1 and Corollary 1 therein); more general theory on symmetry and centre manifolds was developed in [24]. However, the immobility of the symmetric pulse –more widely known as the 'pulse pinning' phenomenon– has to the author's knowledge not been considered in this framework, being a direct consequence of the translational invariance of the underlying system combined with the spatial symmetry of the pulse solution. For an illustration of the statement of Theorem 3.3, see Figure 3.

Proof. We adopt the notation of Theorem 3.1. For the central spectrum (3.2), the reduced spectral subspace $\mathcal{E}'_0$ is spanned by the eigenvectors of the Hopf eigenvalues $\pm i\,\omega_H$, i.e. $\mathcal{E}'_0 = \mathrm{span}\left\{\phi_H, \overline{\phi_H}\right\}$. Therefore, any $\rho_0(\xi, t) \in \mathcal{E}'_0$ can be written as $\rho_0(\xi, t) = A(t)\,\phi_H(\xi) + \overline{A(t)}\,\overline{\phi_H(\xi)}$. Since ϕ_H is even as a function of ξ (see the proof of Lemma 3.2), ρ_0 is even as a function of ξ; in extension, $\Psi(\rho_0)$ is even as a function of ξ. The pulse Γ_h is symmetric (Result 2.3),

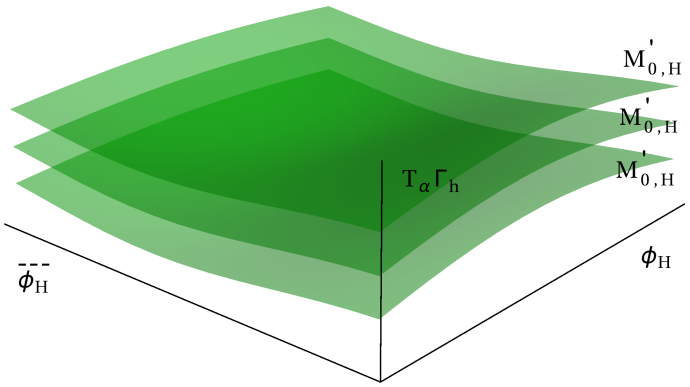

Figure 3: A sketch of the statement of Theorem 3.3 on the foliation of the Hopf centre manifold $\mathcal{M}_{0,H}$. The identical copies of $\mathcal{M}'_{0,H}$ are depicted as green sheets, while the trivial 'stacking' direction spanned by the line of equilibria $\{T_\alpha \Gamma_h,\ \alpha \in \mathbb{R}\}$ is upwards.

so $\Gamma_h(\xi) + \rho(\xi,t) = \Gamma_h(\xi) + \rho_0(\xi,t) + \Psi(\rho_0(\xi,t))$ is even as a function of ξ. That means that $\mathrm{RHS}(\Gamma_h(\xi) + \rho(\xi,t))$ (3.10) is even as a function of ξ. Subsequently, the inner product $\langle \mathrm{RHS}(\Gamma_h(\xi) + \rho(\xi,t)), \frac{\mathrm{d}}{\mathrm{d}\xi}\Gamma_h \rangle$ vanishes identically, since the translational eigenmode $\frac{\mathrm{d}}{\mathrm{d}\xi}\Gamma_h$ is odd in ξ, see the proof of Lemma 3.2. Hence, the right-hand side of (3.13) vanishes. That means that the full dynamics on $\mathcal{M}_{0,H}$ are represented by (3.14), which in turn can be reduced to (3.16). □

Although one would expect, based on the central spectrum (3.2), that the translational eigenmode $\frac{\mathrm{d}}{\mathrm{d}\xi}\Gamma_h$ in general is excitable, Theorem 3.3 shows that this is not the case. In other words, the pulse Γ_h does not move when perturbed under Hopf bifurcation conditions. Theorem 3.3 therefore enables us to 'neglect' the translational eigenmode in the centre manifold expansion. Moreover, this Theorem analytically confirms the numerical results on the 'pinning' of a periodically oscillating pulse in [32], section 5.

4 Expanding the Hopf centre manifold

In this section, we expand the Hopf centre manifold introduced in section 3. Our analysis is based on the approach taken in [20], section 3.4.2 therein.
Based on Theorem 3.1 and Theorem 3.3, we restrict ourselves without loss of generality to $\mathcal{X}' = \mathcal{X} - \mathrm{span}\left\{\frac{\mathrm{d}}{\mathrm{d}\xi}\Gamma_h\right\}$, i.e. we focus on a single leaf of the foliation of the entire centre manifold. As in the proof of Theorem 3.3, we observe that $\mathcal{E}'_0 = \mathrm{span}\left\{\phi_H, \overline{\phi_H}\right\}$. Therefore, any $\rho_0(\xi,t) \in \mathcal{E}'_0$ can be expressed as $\rho_0(\xi,t) = A(t)\,\phi_H(\xi) + \overline{A(t)}\,\overline{\phi_H(\xi)}$. We recall from Theorem 3.1 and Theorem 3.3 that solutions on the centre manifold leaf $\mathcal{M}'_{0,H}$ can be expressed as

$$\begin{pmatrix} U(\xi,t) \\ V(\xi,t) \end{pmatrix} = \Gamma(\xi,t) = \Gamma_h(\xi) + A(t)\,\phi_H(\xi) + \overline{A(t)}\,\overline{\phi_H(\xi)} + \Psi\left(A(t)\,\phi_H(\xi) + \overline{A(t)}\,\overline{\phi_H(\xi)}\right). \tag{4.1}$$

Since our ultimate goal is to make a statement about the (weakly) nonlinear stability of the stationary pulse solution of Result 2.3, we choose to take the explicit parameter dependence

of (2.2) into account. That way, we can analyse what will happen when a continuous parameter change moves the pulse solution through a Hopf bifurcation, such that the pulse becomes linearly unstable. We take μ as our principal bifurcation parameter; however, the analysis is completely analogous when either ν_1 or ν_2 is chosen as bifurcation parameter.
With the parameter dependence taken into account, the parameter dependent normal form for a Hopf bifurcation is given by [20]

$$\frac{\mathrm{d}A}{\mathrm{d}t} = i\,\omega_H\,A + a\,\hat{\mu}\,A + b\,A\,|A|^2 + O\left(A(|\hat{\mu}| + |A|^2)^2\right), \tag{4.2}$$

where $\hat{\mu} = \mu - \mu_H$. To obtain an equation for the normal form coefficients a and b, we need to make a formal expansion of both the local graph of the centre manifold, given by Φ (4.1), and the right-hand side of (2.2) for a perturbation of the pulse solution Γ_h. To start with the latter, we substitute $(U, V) = \Gamma_h + \rho$ in (2.2), yielding

$$\frac{\partial \rho}{\partial t} = \mathcal{L}'\rho + \mathcal{R}(\Gamma_h; \rho). \tag{4.3}$$

with $\mathcal{L}'$ denotes the projection of $\mathcal{L}$ (2.9) onto the subspace $\mathcal{X}'$, see Theorem 3.1. Next, we formally expand the remainder term $\mathcal{R}(\Gamma_h; \rho)$ as

$$\mathcal{R}(\Gamma_h; \rho) = \hat{\mu}\,\mathcal{R}^{\hat{\mu}} + \hat{\mu}\,\mathcal{R}_1^{\hat{\mu}}\rho + \mathcal{R}_2(\rho,\rho) + \mathcal{R}_3(\rho,\rho,\rho) + O\left(|\hat{\mu}|(|\hat{\mu}| + |\rho|^2)\right) + O\left(|\rho|^4\right). \tag{4.4}$$

Note that not every term in the expansion is given explicitly: the terms omitted are not needed for the calculation of the normal form coefficients a and b (4.2). The expansion terms of in (4.4) can be calculated straightforwardly from the Taylor series of their constituents, yielding

$$\mathcal{R}^{\hat{\mu}} = \begin{pmatrix} \nu_1 \frac{\mathrm{d}F_1}{\mathrm{d}U} + \frac{\nu_2}{\varepsilon}\frac{\partial F_2}{\partial U} & \frac{\nu_2}{\varepsilon}\frac{\partial F_2}{\partial V} \\ \frac{\partial G}{\partial U} & \frac{\partial G}{\partial V} \end{pmatrix} \frac{\partial \Gamma_h}{\partial \mu}, \tag{4.5a}$$

$$\mathcal{R}_1^{\hat{\mu}}\rho = \begin{pmatrix} \nu_1 \frac{\mathrm{d}^2F_1}{\mathrm{d}U^2}(\rho)_1 \frac{\partial U_h}{\partial \mu} \\ 0 \end{pmatrix} + \begin{pmatrix} \frac{\nu_2}{\varepsilon} D^2F_2(\rho, \frac{\partial \Gamma_h}{\partial \mu}) \\ D^2G(\rho, \frac{\partial \Gamma_h}{\partial \mu}) \end{pmatrix}, \tag{4.5b}$$

$$\mathcal{R}_2(\rho,\sigma) = \begin{pmatrix} \nu_1 \frac{\mathrm{d}^2F_1}{\mathrm{d}U^2}(\rho)_1(\sigma)_1 \\ 0 \end{pmatrix} + \begin{pmatrix} \frac{\nu_2}{\varepsilon} D^2F_2(\rho,\sigma) \\ D^2G(\rho,\sigma) \end{pmatrix}, \tag{4.5c}$$

$$\mathcal{R}_3(\rho,\sigma,\tau) = \begin{pmatrix} \nu_1 \frac{\mathrm{d}^3F_1}{\mathrm{d}U^3}(\rho)_1(\sigma)_1(\tau)_1 \\ 0 \end{pmatrix} + \begin{pmatrix} \frac{\nu_2}{\varepsilon} D^3F_2(\rho,\sigma,\tau) \\ D^3G(\rho,\sigma,\tau) \end{pmatrix}. \tag{4.5d}$$

Here, $D^2H(\rho,\sigma)$ denotes the symmetric 2-tensor obtained by taking the (total) second derivative of the function $H : \mathbb{R}\times\mathbb{R} \to \mathbb{R}$, where the tensor acts on the pair of vectors (ρ,σ). Equivalently, $D^3H(\rho,\sigma)$ denotes the symmetric 3-tensor obtained by taking the (total) third derivative of H, acting on the vector triplet (ρ,σ,τ). In (4.5), all the (partial) derivatives of $F_{1,2}$ and G are evaluated at the pulse solution $\Gamma_h = (U_h, V_h)^T$ (as in (2.10)). Also, the first resp. second component of a vector ρ is denoted by $(\rho)_1$ resp. $(\rho)_2$.
Now, using the local functional form of the centre manifold (4.1), we specify ρ as

$$\rho = A(t)\,\phi_H(\xi) + \overline{A(t)}\,\overline{\phi_H(\xi)} + \Psi\left(A(t)\,\phi_H(\xi) + \overline{A(t)}\,\overline{\phi_H(\xi)}\right). \tag{4.6}$$

Next, we expand $\Psi\left(A(t)\,\phi_H(\xi) + \overline{A(t)}\,\overline{\phi_H(\xi)}\right)$ in a power series in $\hat{\mu}$ and $A, \overline{A}$ as

$$\begin{aligned} \Psi\left(A(t)\,\phi_H(\xi) + \overline{A(t)}\,\overline{\phi_H(\xi)}\right) \;=\; & A^2\Psi_{20} + A\,\overline{A}\Psi_{11} + \overline{A}^2\overline{\Psi_{20}} \\ & + A^3\Psi_{30} + A^2\overline{A}\Psi_{21} + A\,\overline{A}^2\overline{\Psi_{21}} + \overline{A}^3\overline{\Psi_{30}} + O\left(|A|^4\right) \\ & + \hat{\mu}\Psi_{00}^{\hat{\mu}} + \hat{\mu}A\Psi_{10}^{\hat{\mu}} + \hat{\mu}\overline{A}\,\overline{\Psi_{10}^{\hat{\mu}}} + O\left(|\hat{\mu}|(|\hat{\mu}| + |A|^2)\right). \end{aligned} \tag{4.7}$$

Combining (4.7) with (4.6) and substituting the result in (4.3), one can use (4.4) and the normal form (4.2)to identify the expansion terms by increasing order. This procedure yields for the first and nonmixed second order terms

$$O(\hat{\mu}): \qquad \mathcal{L}'\,\Psi_{00}^{\hat{\mu}} = -\mathcal{R}^{\hat{\mu}}, \tag{4.8a}$$

$$O\left(A^2\right): \qquad (\mathcal{L}' - 2\,i\,\omega_H)\,\Psi_{20} = -\mathcal{R}_2(\phi_H, \phi_H), \tag{4.8b}$$

$$O\left(A\overline{A}\right): \qquad \mathcal{L}'\,\Psi_{11} = -2\mathcal{R}_2(\phi_H, \overline{\phi_H}). \tag{4.8c}$$

Note that, since we have restricted our analysis to one leaf of the foliation given in Theorem 3.3, and hence work in the space $\mathcal{X}'$, which is the complement of the span of the trivial eigenmode $\frac{\mathrm{d}}{\mathrm{d}\xi}\Gamma_h$, we see that the operator $\mathcal{L}'$ is invertible in this subspace and hence both $\Psi_{00}^{\hat{\mu}}$ and Ψ_{11} are uniquely determined by (4.8a) resp. (4.8c). Moreover, since we assumed the central spectrum of $\mathcal{L}$ to be given by (3.2), we see that

$$\sigma'_{0,H} = \{\pm i\,\omega_H\}\,. \tag{4.9}$$

Therefore, the operator $(\mathcal{L}' - 2\,i\,\omega_H)$ is invertible as well, thereby uniquely determining Ψ_{20} by (4.8b).
Returning to the results of the substitution procedure, identification of the the third order and mixed second order terms yields

$$O(\hat{\mu}A): \qquad (\mathcal{L}' - i\,\omega_H)\,\Psi_{10}^{\hat{\mu}} = a\,\phi_H - \mathcal{R}_1^{\hat{\mu}}\phi_H - 2\mathcal{R}_2\left(\phi_H, \Psi_{00}^{\hat{\mu}}\right), \tag{4.10a}$$

$$O\left(A|A|^2\right): \qquad (\mathcal{L}' - i\,\omega_H)\,\Psi_{21} = b\,\phi_H - 2\mathcal{R}_2\left(\phi_H, \Psi_{11}\right) - 2\mathcal{R}_2\left(\overline{\phi_H}, \Psi_{20}\right) - 3\mathcal{R}_3\left(\phi_H, \phi_H, \overline{\phi_H}\right) \tag{4.10b}$$

Since we assume the Hopf eigenvalues $\pm i\,\omega_H$ to be simple, such that the Hopf bifurcation has codimension 1, the equations for $\Psi_{10}^{\hat{\mu}}$ and Ψ_{21} can be solved if and only if the appropriate solvability condition is satisfied. In both cases, the solvability condition demands that the right-hand sides of (4.10a) and (4.10b) are orthogonal to the kernel of the adjoint operator $(\mathcal{L}'^{*} + i\,\omega_H)$. The kernel of the adjoint $(\mathcal{L}'^{*} + i\,\omega_H)$ is also one-dimensional, and $\mathcal{L}'^{*}$ is real, so we can introduce the eigenfunction ϕ_H^{*} for which

$$\mathcal{L}'^{*}\phi_H'^{*} = i\,\omega_H\,\phi_H'^{*}. \tag{4.11}$$

The solvability condition for (4.10a) and (4.10b) then yields the following equations for a and b:

$$a = \frac{\langle \mathcal{R}_1^{\hat{\mu}}\phi_H + 2\mathcal{R}_2\left(\phi_H, \Psi_{00}^{\hat{\mu}}\right), \overline{\phi_H'^{*}}\rangle}{\langle \phi_H, \overline{\phi_H'^{*}}\rangle}, \tag{4.12}$$

$$b = \frac{\langle 2\mathcal{R}_2\left(\phi_H, \Psi_{11}\right) + 2\mathcal{R}_2\left(\overline{\phi_H}, \Psi_{20}\right) + 3\mathcal{R}_3\left(\phi_H, \phi_H, \overline{\phi_H}\right), \overline{\phi_H'^{*}}\rangle}{\langle \phi_H, \overline{\phi_H'^{*}}\rangle}. \tag{4.13}$$

In the next section, the constituents of (4.12) and (4.13) will be treated in more detail.

It is worthwhile to note that the theory presented in section 3 and 4 is nonperturbative in the small parameter ε. The mere fact that, for ε small enough, the existence of a pulse solution to (2.2) can be proven, only provides the necessary input for the setup of the centre manifold theory of sections 3 and 4. The next section will see the return of the leading order expressions for the pulse and its eigenfunctions, as established in Results 2.3 and 2.4.

5 Using the scale separated pulse structure

In this section, the different ingredients needed to calculate the Hopf normal form coefficents a (4.12) and b (4.13) will be treated in a systematic fashion. The scale separated structure of the underlying system (2.2), of the pulse solution (Result 2.3) and the Hopf eigenfunctions (Result 2.4) will prove instrumental in obtaining explicit leading order expressions for a and b.

5.1 The adjoint eigenfunction $\phi_H'^*$

To obtain a leading order expression for the adjoint eigenfunction $\phi_H'^*$, we study the adjoint operator $\mathcal{L}'^*$.
Combining the definition of $\mathcal{L}$ (2.9) with that of the scaling matrix S used in the definition of the inner product (3.4), we see that $\mathcal{L}$ can be written as

$$\mathcal{L} = S^{-2}\frac{\mathrm{d}^2}{\mathrm{d}\xi^2} - \mathcal{A}. \tag{5.1}$$

Now,

$$\begin{aligned}
\langle \phi, \mathcal{L}^*\psi\rangle = \langle \mathcal{L}\phi, \psi\rangle &= \int_{\mathbb{R}} (\mathcal{L}\phi)^T S\overline{\psi}\,\mathrm{d}\xi \\
&= \int_{\mathbb{R}} \left(S^{-2}\frac{\mathrm{d}^2}{\mathrm{d}\xi^2}\phi\right)^T S\overline{\psi} - (\mathcal{A}\phi)^T S\overline{\psi}\,\mathrm{d}\xi \\
&= \int_{\mathbb{R}} \left(\frac{\mathrm{d}^2}{\mathrm{d}\xi^2}\phi\right)^T S^{-2}S\overline{\psi} - \phi^T\mathcal{A}^T S\overline{\psi}\,\mathrm{d}\xi \\
&= \int_{\mathbb{R}} \phi^T S^{-2}S\frac{\mathrm{d}^2}{\mathrm{d}\xi^2}\overline{\psi} - \phi^T S\, S^{-1}\mathcal{A}^T S\overline{\psi}\,\mathrm{d}\xi \quad \text{(see Remark 5.2)} \\
&= \int_{\mathbb{R}} \phi^T S\overline{\left[S^{-2}\frac{\mathrm{d}^2}{\mathrm{d}\xi^2} - S^{-1}\mathcal{A}^T S\right]\psi}\,\mathrm{d}\xi,
\end{aligned}$$

so

$$\mathcal{L}^* = S^{-2}\frac{\mathrm{d}^2}{\mathrm{d}\xi^2} - S^{-1}\mathcal{A}^T S. \tag{5.2}$$

Using (2.10),

$$S^{-1}\mathcal{A}^T S = \left.\begin{pmatrix} \mu - \nu_1\frac{\mathrm{d}F_1}{\mathrm{d}U} - \frac{\nu_2}{\varepsilon}\frac{\partial F_2}{\partial U} & -\frac{1}{\varepsilon}\frac{\partial G}{\partial U} \\ -\nu_2\frac{\partial F_2}{\partial V} & 1 - \frac{\partial G}{\partial V}\end{pmatrix}\right|_{(U,V)=(U_h(\xi),V_h(\xi))}. \tag{5.3}$$

We see that $\mathcal{L}^*$ has the same scale separated structure as $\mathcal{L}$, with only the roles of $\nu_2\frac{\partial F_2}{\partial V}$ and $\frac{\partial G}{\partial U}$ reversed. Therefore, Result 2.4 applies to eigenfunctions of $\mathcal{L}^*$, in a slightly updated form. Since the diagonal entries of $\mathcal{A}$ are the same as those of $S^{-1}\mathcal{A}^T S$, the leading order slow and fast linear operators associated to $\mathcal{L}^*$ coincide with those of $\mathcal{L}$, i.e. $(\mathcal{L}^*)_s(x) = \mathcal{L}_s(x)$ and $(\mathcal{L}^*)_f(\xi) = \mathcal{L}_f(\xi)$, as given in (2.13) resp. (2.12). The leading order fast nonhomogeneous Sturm-Liouville problem for $\mathcal{L}^*$ (compare (2.14)) is

$$\left(\mathcal{L}_f^* - \lambda\right)v = -\nu_2\frac{\partial F_2}{\partial V}(u_*, v_{f,h}(\xi;u_*)), \quad \xi\in\mathbb{R}. \tag{5.4}$$

Analogous to section 2.2, we denote the unique bounded solution to (5.4) by $v_{\text{in}}^*(\xi;\lambda)$. Using these observations, we state the existence and leading order structure of $\phi_H'^*$ in a manner similar to Result 2.4:

Lemma 5.1. *Let $\mathcal{L}'^*$ be the adjoint of $\mathcal{L}'$, as defined in Theorem 3.1. There exists a unique, bounded, integrable function $\phi_H'^* : \mathbb{R}\to\mathbb{C}^2$ such that $\mathcal{L}'^*(\xi;\varepsilon)\,\phi_H'^*(\xi;\varepsilon) = i\,\omega_H\,\phi_H'^*(\xi;\varepsilon)$. Furthermore, there are $O(1)$ constants $C_{1,2}$ such that the following holds:*

- $\phi_H'^*(\xi;\varepsilon) = \phi_H(\xi;\varepsilon) + C_1 e^{-|C_2|\xi}$ *for* $\xi > \varepsilon^{-\frac{1}{4}}$;
- $\phi_H'^*(\xi;\varepsilon) = \phi_H'^*(-\xi;\varepsilon)$ *for* $\xi < -\varepsilon^{-\frac{1}{4}}$;
- $\phi_H'^*(\xi;\varepsilon) = u_{s,-}(0; i\,\omega_H)\begin{pmatrix} 1 \\ v_{\text{in}}^*(\xi; i\,\omega_H)\end{pmatrix} + O(\varepsilon^{\frac{3}{4}})$ *for* $\xi \in I_f$.

Here, $v_{in}^*(\xi; i\,\omega_H)$ *is the unique bounded solution to* (5.4) *for* $\lambda = i\,\omega_H$*, and* $u_{s,-}$ *is as in Result 2.4.*

Proof. Since F_2 and G obey equivalent conditions, see Assumptions 2.2, (A3) and (A4), the theory developed in [11], section 3 can be directly applied to $\mathcal{L}^*$, yielding Hopf eigenfunctions ϕ_H^*, $\overline{\phi_H^*}$ with the scale separated structure as described in Result 2.4. Outside I_f, the leading order behaviour of ϕ_H^* coincides with that of ϕ_H, since $(\mathcal{L}^*)_s(x) = \mathcal{L}_s(x)$. Moreover, since ϕ_H^* is an even function, we can invoke Lemma 3.2 to conclude that $\phi_H^* \in \mathcal{X}'$. Therefore, ϕ_H^* is also the eigenfunction of the reduced adjoint operator $\mathcal{L}'^*$ for the eigenvalue $i\,\omega_H$, allowing us to identify $\phi_H^* = \phi_H'^*$. □

Remark 5.2. In the derivation of $\mathcal{L}^*$ (5.2), we used partial integration to 'transfer' the differential operator $\frac{\mathrm{d}^2}{\mathrm{d}\xi^2}$ from ϕ to ψ. Since every function ϕ we consider in this paper is exponentially decreasing as $\xi \to \pm\infty$ and sufficiently smooth, this operation is justified in the present context. However, this is not necessarily true for every function in the function space $\mathcal{X}$ (3.3). We therefore implicitly restrict ourselves to the subset of $\mathcal{X}$ where the adjoint of $\mathcal{L}$ can be identified with the expression given in (5.2). One could also opt for finding a more suitable, restricted function space to work in. However, this falls beyond the scope of this paper.

5.2 Solving inhomogeneous equations involving $\mathcal{L}'$

We first derive a general result on solving equations of the following form:

$$(\mathcal{L}' - \kappa)\,\psi = \begin{pmatrix} A(\varepsilon\xi) + \frac{1}{\varepsilon}B((\varepsilon\xi,\xi) \\ C(\varepsilon\xi,\xi)\end{pmatrix}, \tag{5.5}$$

where A, B, C are exponentially decreasing as their argument tends to $\pm\infty$, i.e.

$$\exists\, C^A_{1,2,3,4} \in \mathbb{R} \quad : \quad \begin{cases} A(x) \rightsquigarrow C_1^A\, e^{-|C_2^A|x} & \text{as} \quad x \to \infty \\ A(x) \rightsquigarrow C_3^A\, e^{|C_4^A|x} & \text{as} \quad x \to -\infty \end{cases},$$
$$\exists\, C^B_{1,2,3,4} \in \mathbb{R} \quad : \quad \begin{cases} B(\varepsilon\xi,\xi) \rightsquigarrow C_1^B\, e^{-|C_2^B|\xi} & \text{as} \quad \xi \to \infty \\ B(\varepsilon\xi,\xi) \rightsquigarrow C_3^B\, e^{|C_4^B|\xi} & \text{as} \quad \xi \to -\infty \end{cases},$$

and analogously for $C(\varepsilon\xi,\xi)$.

For the moment, consider (5.5) extended to $\mathcal{X}$, i.e. with $\mathcal{L}$ replacing $\mathcal{L}'$. Using the definition of $\mathcal{L}$ (2.9), this extended equation for $\psi = (u, v)^T$ is then

$$\left[\begin{pmatrix}\varepsilon^{-2} & 0 \\ 0 & 1\end{pmatrix}\frac{\mathrm{d}^2}{\mathrm{d}\xi^2} - (\kappa + \mathcal{A}(\xi;\varepsilon))\right]\begin{pmatrix} u \\ v\end{pmatrix} = \begin{pmatrix} A(\varepsilon\xi) + \frac{1}{\varepsilon}B((\varepsilon\xi,\xi) \\ C(\varepsilon\xi,\xi)\end{pmatrix} \tag{5.6}$$

In [11], the scale separated structure of the homogeneous version of (5.6) was used to obtain Sturm-Liouville type equations for the components u and v, see also section 2.2. The same line of reasoning can be straightforwardly applied to (5.6). For more information on the order estimates and detailed arguments on the validity of the approach, the reader is referred to[11].

5.2.1 Equation (5.6) on the fast interval I_f

Using leading order analysis analogous to that in [11], we see that on the fast interval I_f (2.4),

$$u = u(0) + O\left(\varepsilon^{\frac{3}{4}}\right) \quad \text{for} \quad \xi \in I_f, \tag{5.7}$$

$$\frac{\mathrm{d}^2}{\mathrm{d}\xi^2} v - \left[1 + \kappa - \frac{\partial G}{\partial V}\right] v = -\frac{\partial G}{\partial U} u(0) + C(0,\xi) + O\left(\varepsilon^{\frac{3}{4}}\right), \tag{5.8}$$

where the partial dervatives of G are, as usual, evaluated at $(U, V) = (U_h, V_h) = (u_*, v_{f,h}(\xi; u_*)) + O\left(\varepsilon^{\frac{3}{4}}\right)$ on I_f, see Result 2.3. We want to solve the inhomogeneous Sturm-Liouville equation (5.8) on $\mathbb{R}$ with boundary conditions $\lim_{\xi\to\pm\infty} v(\xi) = 0$, using its homogeneous version

$$\frac{\mathrm{d}^2}{\mathrm{d}\xi^2} v - \left[1 + \kappa - \frac{\partial G}{\partial V}\right] v = 0, \quad \lim_{\xi\to\pm\infty} v(\xi) = 0. \tag{5.9}$$

Note that (5.9) can be phrased in terms of $\mathcal{L}_f(\xi)$ (2.12) as $\left(\mathcal{L}_f(\xi) - \kappa\right) v = 0$. Detailed analysis of this fast reduced eigenvalue problem and information on its spectrum can be found in [11].

In this paper, we consider two cases:

a) Equation (5.9) admits no nontrivial solution. By the Fredholm alternative, (5.8) has a unique bounded solution $\hat{v}(\xi)$. Since $\frac{\partial G}{\partial V}$ vanishes as $\xi \to \pm\infty$, we can find two linearly independent solutions $v_{\mathrm{L/R}}(\xi)$ to (5.9) for which $v_{\mathrm{L}}(\xi) \rightsquigarrow \hat{c}_{\mathrm{L}} e^{\sqrt{1+\kappa}\xi}$ as $\xi \to -\infty$ and $v_{\mathrm{R}}(\xi) \rightsquigarrow \hat{c}_{\mathrm{R}} e^{-\sqrt{1+\kappa}\xi}$ as $\xi \to -\infty$ (see also Lemma 3.2 in [11]). Using variation of parameters (or using Green's function), we can express $\hat{v}$ in terms of $v_{\mathrm{L/R}}$ as

$$\hat{v}(\xi) = v_{\mathrm{R}}(\xi) \int_{-\infty}^{\xi} v_{\mathrm{L}}(\hat{\xi}) \left[\frac{\partial G}{\partial U} u(0) - C(0,\hat{\xi})\right] \mathrm{d}\hat{\xi} + v_{\mathrm{L}}(\xi) \int_{\xi}^{\infty} v_{\mathrm{R}}(\hat{\xi}) \left[\frac{\partial G}{\partial U} u(0) - C(0,\hat{\xi})\right] \mathrm{d}\hat{\xi}, \tag{5.10a}$$

$$:= u(0)\, \hat{v}_1(\xi) + \hat{v}_2(\xi) \tag{5.10b}$$

where $v_{\mathrm{L/R}}$ are normed such that the Wronskian $W(v_{\mathrm{R}}, v_{\mathrm{L}}) = 1$.

b) The parameter κ is zero. In this case, the function $v_1(\xi) = \frac{\mathrm{d}}{\mathrm{d}\xi} v_{f,h}(\xi; u_*)$ solves the homogeneous problem (5.9). The other (unbounded) solution $v_2(\xi)$ to equation (5.9) would then formally be given by

$$v_1(\xi) \int^{\xi} \frac{1}{v_1(\hat{\xi})^2}\, \mathrm{d}\hat{\xi}.$$

One could regard the integral as an antiderivative, which, in some applications, might be calculated directly. Otherwise, this integral is ill-defined whatever the choice of lower limit, since the integrand diverges as $\hat{\xi} \to 0$. Note that the total expression, being the product of $v_1(\xi)$ and the singular integral, is smooth at the origin.
Since the singularity of the integrand at the origin prevents us from 'integrating through' the origin, we choose to define the unbounded solution to (5.9) as

$$v_2(\xi; a) = \begin{cases} v_1(\xi) \int_{-a}^{\xi} \frac{1}{v_1(\hat{\xi})^2}\, \mathrm{d}\hat{\xi} & \text{for} \quad \xi < 0, \\ -v_1(\xi) \int_{\xi}^{a} \frac{1}{v_1(\hat{\xi})^2}\, \mathrm{d}\hat{\xi} & \text{for} \quad \xi > 0. \end{cases} \tag{5.11}$$

Whatever the choice of a, $v_2(\xi; a)$ is an even function of ξ. Also, it solves the homogeneous problem (5.9) for $\kappa = 0$ at both sides of the origin. However, we still need to check that v_2 is smooth at $\xi = 0$. Using the fact that $v_{f,h}(\xi; u_*)$ is a solution to the fast reduced system (2.5) which is homoclinic to the origin (Assumptions 2.2, (A5)), integrating (2.5) once yields

$$\left(\frac{\mathrm{d}}{\mathrm{d}\xi} v_{f,h}\right)^2 = v_{f,h}^2 - 2 \int_0^{v_{f,h}} G(u_*, v)\, \mathrm{d}v. \tag{5.12}$$

Using (5.12), we see that

$$\lim_{\xi\uparrow 0} v_2(\xi;a) = \lim_{\xi\downarrow 0} v_2(\xi;a) = \frac{-1}{v_{f,h}(0;u_*) - G(u_*, v_{f,h}(0;u_*))} \tag{5.13}$$

so $v_2(\xi;a)$ is continuous at the origin. However, for an even function such as v_2 to be differentiable at the origin, we need to make sure that both $\lim_{\xi\uparrow 0} \frac{\mathrm{d}v_2}{\mathrm{d}\xi}$ and $\lim_{\xi\downarrow 0} \frac{\mathrm{d}v_2}{\mathrm{d}\xi}$ vanish at $\xi = 0$.

Lemma 5.3. *Consider*

$$f(a) = \frac{1}{v_1(a)} + \int_0^a \left(1 - \frac{\partial G}{\partial V}(u_*, v_{f,h}(\xi;u_*))\right) v_1(\xi) \int_\xi^a \frac{1}{v_1(\hat{\xi})^2}\, d\hat{\xi}\, d\xi. \tag{5.14}$$

There exists a unique value $a_* > 0$ such that $f(a_*) = 0$.

Proof. Since the integrand in (5.14) is bounded, and $v_1(\xi) \to 0$ as $\xi \downarrow 0$, we see that

$$f(a) \rightsquigarrow \frac{1}{v_1(a)} \quad \text{as} \quad a \downarrow 0,$$

so $f(a) \to -\infty$ as $a \downarrow 0$. Using integration by parts, $f(a)$ can be represented as

$$f(a) = \lim_{\varepsilon\downarrow 0} -\frac{\mathrm{d}v_1}{\mathrm{d}\xi}(\varepsilon) \int_\varepsilon^a \frac{1}{v_1(\hat{\xi})^2}\, \mathrm{d}\hat{\xi} + \frac{1}{v_1(\varepsilon)},$$

so

$$\frac{\mathrm{d}f}{\mathrm{d}a} = \lim_{\varepsilon\downarrow 0} -\frac{\mathrm{d}v_1}{\mathrm{d}\xi}(\varepsilon)\frac{1}{v_1(a)^2} = -\frac{\mathrm{d}v_1}{\mathrm{d}\xi}(0)\frac{1}{v_1(a)^2}. \tag{5.15}$$

and hence $\frac{\mathrm{d}f}{\mathrm{d}a} > 0$ for all $a > 0$. Moreover, since $-\frac{\mathrm{d}v_1}{\mathrm{d}\xi}(0)$ is strictly positive and $|v_1(a)|$ is bounded from above, there exists a constant $C > 0$ such that $\frac{\mathrm{d}f}{\mathrm{d}a} > C$ for all $a > 0$. Therefore, $f(a)$ is strictly monotonically increasing, and its derivative is bounded away from zero: hence, $f(a) \to \infty$ as $a \to \infty$. We conclude that there exists a unique value $a_* > 0$ such that $f(a_*) = 0$. □

Corollary 5.4. *There exists a unique $a_* > 0$ such that the function $v_2(\xi;a_*)$ (5.11) is continuously differentiable at the origin.*

Proof. Consider $v_2(\xi;a)$ (5.11) for $\xi > 0$. Integration by parts yields

$$\lim_{\xi\downarrow 0} \frac{\mathrm{d}v_2}{\mathrm{d}\xi} = \frac{1}{v_1(a)} + \int_0^a \frac{\mathrm{d}^2 v_1}{\mathrm{d}\xi^2}(\xi) \int_\xi^a \frac{1}{v_1(\hat{\xi})^2}\, \mathrm{d}\hat{\xi}\, \mathrm{d}\xi.$$

Taking the derivative to ξ of (2.5), we see that

$$\frac{\mathrm{d}^2 v_1}{\mathrm{d}\xi^2}(\xi) = \left(1 - \frac{\partial G}{\partial V}(u_*, v_{f,h}(\xi;u_*))\right) v_1;$$

therefore, $\lim_{\xi\downarrow 0} \frac{\mathrm{d}v_2}{\mathrm{d}\xi} = f(a)$. □

We conclude that $v_2(\xi;a_*)$ is continuously differentiable at the origin, obeys the second order differential equation (5.9) on $\mathbb{R} \setminus \{0\}$ and is therefore smooth in $\xi = 0$. Therefore, $v_2(\xi;a_*)$ obeys the equation (5.9) on the entire real line, and is therefore well-defined as a solution to the homogeneous problem (5.9).

As in the case a) (5.10), we can express the solution v_0 to the nonhomogeneous problem (5.8) in terms of $v_{1,2}$ as

$$v_0(\xi) = -v_1(\xi) \int_\xi^b v_2(\hat{\xi};a_*) \left[\frac{\partial G}{\partial U} u(0) - C(0,\hat{\xi})\right] \mathrm{d}\hat{\xi} - v_2(\xi;a_*) \int_{-\infty}^\xi v_1(\hat{\xi}) \left[\frac{\partial G}{\partial U} u(0) - C(0,\hat{\xi})\right] \mathrm{d}\hat{\xi},$$

since the Wronskian of $v_{1,2}$ yields $W(v_1, v_2) = 1$. The integral limit b is still undetermined, due to the fact that the homogeneous problem (5.9) admits a nontrivial solution v_1. Therefore, v_0 can be uniquely determined up to a multiple of v_1. For future convenience, we choose b such that v_0 is an even function of ξ, i.e. such that

$$\int_{-b}^{b} v_2(\xi; a_*) \left[\frac{\partial G}{\partial U} u(0) - C(0, \hat{\xi}) \right] \mathrm{d}\xi = 0. \tag{5.16}$$

Although for different choices of G and C this equation may have several solutions for b, it is clear that choosing $b = 0$ is sufficient to satisfy (5.16). We therefore choose to gauge v_0 such that it is uniquely represented by

$$\begin{aligned} v_0(\xi) &= -v_1(\xi) \int_{\xi}^{0} v_2(\hat{\xi}; a_*) \left[\frac{\partial G}{\partial U} u(0) - C(0, \hat{\xi}) \right] \mathrm{d}\hat{\xi} - v_2(\xi; a_*) \int_{-\infty}^{\xi} v_1(\hat{\xi}) \left[\frac{\partial G}{\partial U} u(0) - C(0, \hat{\xi}) \right] \mathrm{d}\hat{\xi} \\ &:= u(0)\, v_{0,1}(\xi) + v_{0,2}(\xi). \end{aligned} \tag{5.17a}$$

5.2.2 Equation (5.6) outside the fast interval I_f

Again basing ourselves on [11], we see that outside the fast interval I_f (2.4), both B and C are exponentially small in ε. Moreover, any bounded solution to (5.8) is also exponentially small outside I_f. Therefore, in $x = \varepsilon\xi$,

$$\frac{\mathrm{d}^2}{\mathrm{d}x^2} u - \left[\mu + \kappa - \nu_1 \frac{\mathrm{d}F_1}{\mathrm{d}U} \right] u = A(x) \quad \text{outside } I_f \tag{5.18}$$

up to exponentially small terms in ε, where $\frac{\mathrm{d}F_1}{\mathrm{d}U}$ is evaluated at $U = U_h(\xi) = u_{s,0}(\pm(x_* + x))$ outside I_f, see Result 2.3. We obtain two inhomogeneous Sturm-Liouville equations, left and right of the fast interval I_f:

$$\frac{\mathrm{d}^2}{\mathrm{d}x^2} u - \left[\mu + \kappa - \nu_1 \frac{\mathrm{d}F_1}{\mathrm{d}U} \left(u_{s,0}(x_* + x) \right) \right] u = A(x), \quad x > 0, \tag{5.19a}$$

$$\frac{\mathrm{d}^2}{\mathrm{d}x^2} u - \left[\mu + \kappa - \nu_1 \frac{\mathrm{d}F_1}{\mathrm{d}U} \left(u_{s,0}(x_* - x) \right) \right] u = A(x), \quad x < 0. \tag{5.19b}$$

We consider the right equation (5.19a), whose homogeneous version is given by

$$\frac{\mathrm{d}^2}{\mathrm{d}x^2} u - \left[\mu + \kappa - \nu_1 \frac{\mathrm{d}F_1}{\mathrm{d}U} \left(u_{s,0}(x_* + x) \right) \right] u = 0, \quad x > 0. \tag{5.20}$$

Since $\lim_{x\to\infty} \frac{\mathrm{d}F_1}{\mathrm{d}U} \left(u_{s,0}(x_* + x) \right) = 0$, we can find two linearly independent solutions $u_\pm(x)$ to (5.20) for which $u_\pm(x) \rightsquigarrow c_\pm e^{\pm\sqrt{\mu+\kappa}\, x}$ as $x \to \infty$. Note that (5.20) can be phrased in terms of $\mathcal{L}_s(x)$ (2.13) as $(\mathcal{L}_s(x) - \kappa)\, u = 0$; detailed analysis of this slow reduced eigenvalue problem and information on its spectrum can be found in [11].

We want to solve the Sturm-Liouville problem given by (5.19a) with the boundary condition $\lim_{x\to\infty} u(x) = 0$, while the boundary condition at $x = 0$ stays open. Since $u_-(x)$ solves the associated homogeneous problem, we already know that the solution the inhomogeneous problem will be determined up to a multiple of u_-. Using variation of parameters, we can express the solution u_R to the nonhomogeneous equation (5.19a) in terms of $u_\pm$ as

$$u_\mathrm{R}(x) = u_-(x) \int_0^x u_+(\hat{x}) \left[-A(\hat{x}) \right] \mathrm{d}\hat{x} + u_+(x) \int_x^\infty u_-(\hat{x}) \left[-A(\hat{x}) \right] \mathrm{d}\hat{x} + c_\mathrm{R} u_-(x), \tag{5.21}$$

where $u_\pm$ are normed such that $W(u_-, u_+) = 1$. Note that the open boundary condition at $x = 0$ can be incorporated in the gauge freedom given by $c_\mathrm{R} u_-(x)$. Since the homogeneous problem

(5.20) is symmetric in x, we can express the solution u_{L} to (5.19b) for which $\lim_{x\to-\infty} u_{\mathrm{L}}(x) = 0$ in terms of $u_\pm$ as

$$u_{\mathrm{L}}(x) = u_+(-x)\int_{-\infty}^{x} u_-(-\hat{x})\,[-A(\hat{x})]\;\mathrm{d}\hat{x} + u_-(-x)\int_{x}^{0} u_+(-\hat{x})\,[-A(\hat{x})]\;\mathrm{d}\hat{x} + c_{\mathrm{L}}u_-(-x). \tag{5.22}$$

5.2.3 Equation (5.6) on the entire real line

We can now combine the results of the previous sections 5.2.1 and 5.2.2 to obtain leading order expressions for bounded solutions to (5.6). As in section 5.2.1, we consider two cases:

a) The operator $(\mathcal{L}-\kappa)$ is invertible. It follows that (5.6) has a unique solution. To obtain a leading order expression for that solution, we combine the results of section 5.2.1, case a) and section 5.2.2. In order to fix the gauge in the solutions left and right of the fast interval I_f, we track the change of the derivative of the slow variable u over that fast interval. In [11], this technique was used to obtain a leading order Evans function for the stability problem associated to the pulse from Result 2.3.
We calculate

$$\begin{aligned}\Delta_{I_f}\frac{\mathrm{d}u}{\mathrm{d}\xi} &= \int_{I_f}\frac{\mathrm{d}^2u}{\mathrm{d}\xi^2}\,\mathrm{d}\xi \\ &= \varepsilon\int_{I_f} -\nu_2\frac{\partial F_2}{\partial U}u(0) - \nu_2\frac{\partial F_2}{\partial V}\left(u(0)\,\hat{v}_1(\xi)+\hat{v}_2(\xi)\right) + B(0,\xi)\,\mathrm{d}\xi + O\left(\varepsilon^{\frac{3}{2}}\right)\end{aligned} \tag{5.23}$$

using (5.6), combined with leading order expressions (5.7) and (5.10) for u and v on I_f. The partial derivatives of F_2 are evaluated at $(U,V) = (u_*, v_{f,h}(\xi;u_*))$. On the other hand, we have

$$\frac{\mathrm{d}u}{\mathrm{d}\xi}\left(\varepsilon^{-\frac{1}{4}}\right) = \varepsilon\frac{\mathrm{d}u}{\mathrm{d}x}\left(\varepsilon^{\frac{3}{4}}\right) = \varepsilon\frac{\mathrm{d}u_{\mathrm{R}}}{\mathrm{d}x}(0) + O\left(\varepsilon^{\frac{7}{4}}\right)$$

and vice versa on the left side of I_f. Using the explicit expressions (5.21) and (5.22), we therefore obtain

$$\begin{aligned}\Delta_{I_f}\frac{\mathrm{d}u}{\mathrm{d}\xi} &= \varepsilon\left(\frac{\mathrm{d}u_{\mathrm{R}}}{\mathrm{d}x}(0) - \frac{\mathrm{d}u_{\mathrm{L}}}{\mathrm{d}x}(0)\right) + O\left(\varepsilon^{\frac{7}{4}}\right) \\ &= \varepsilon\left(\frac{\mathrm{d}u_-}{\mathrm{d}x}(0)\int_{-\infty}^{0} u_+(-\hat{x})\,[-A(\hat{x})]\;\mathrm{d}\hat{x} + \frac{\mathrm{d}u_+}{\mathrm{d}x}(0)\int_0^{\infty} u_-(\hat{x})\,[-A(\hat{x})]\;\mathrm{d}\hat{x}\right. \\ &\qquad \left. +(c_{\mathrm{L}}+c_{\mathrm{R}})\frac{\mathrm{d}u_-}{\mathrm{d}x}(0)\right) + O\left(\varepsilon^{\frac{7}{4}}\right).\end{aligned} \tag{5.24}$$

Combining this with the fact that u is constant to leading order in I_f, i.e.

$$u(0) = u_{\mathrm{R}}(0) = u_+(0)\int_0^{\infty} u_-(\hat{x})\,[-A(\hat{x})]\;\mathrm{d}\hat{x} + c_{\mathrm{R}}u_-(0), \tag{5.25a}$$

$$u(0) = u_{\mathrm{L}}(0) = u_-(0)\int_{-\infty}^{0} u_+(-\hat{x})\,[-A(\hat{x})]\;\mathrm{d}\hat{x} + c_{\mathrm{L}}u_-(0), \tag{5.25b}$$

and that $u_\pm$ are scaled such that the Wronskian equals 1, i.e.

$$u_-(0)\frac{\mathrm{d}u_+}{\mathrm{d}x}(0) - \frac{\mathrm{d}u_-}{\mathrm{d}x}(0)u_+(0) = 1, \tag{5.26}$$

allows us to express $c_{\mathrm{L/R}}$ as

$$c_{\mathrm{L}} + \int_{-\infty}^{0} u_+(-\hat{x})\,[-A(\hat{x})]\;\mathrm{d}\hat{x} = c_{\mathrm{R}} + \frac{u_+(0)}{u_-(0)} \int_0^{\infty} u_-(\hat{x})\,[-A(\hat{x})]\;\mathrm{d}\hat{x}$$
$$= -\frac{\frac{1}{u_-(0)} \int_0^{\infty} u_-(\hat{x})\,[-A(\hat{x})]\;\mathrm{d}\hat{x} + \int_{-\infty}^{\infty} \nu_2 \frac{\partial F_2}{\partial V} \hat{v}_2(\xi) - B(0,\xi)\,\mathrm{d}\xi}{u_-(0) \int_{-\infty}^{\infty} \nu_2 \frac{\partial F_2}{\partial U} + \nu_2 \frac{\partial F_2}{\partial V} \hat{v}_1(\xi)\,\mathrm{d}\xi + 2\frac{\mathrm{d}u_-}{\mathrm{d}x}(0)} \tag{5.27}$$

up to order $O\left(\varepsilon^{\frac{3}{4}}\right)$. We summarize the above results in the following Lemma:

Lemma 5.5. *Assume that $(\mathcal{L} - \kappa)$ is invertible. Then* (5.6) *has a unique bounded solution $\psi = (u, v)^T$, for which there are $C_{1,2} \in \mathbb{R}$ such that the following holds:*

- $\psi(\xi) = \begin{pmatrix} u_{\mathrm{R}}(\varepsilon\xi) \\ 0 \end{pmatrix} + C_1 e^{-|C_2|\xi}$ *for* $\xi > \varepsilon^{-\frac{1}{4}}$;
- $\psi(\xi) = \begin{pmatrix} u_{\mathrm{L}}(\varepsilon\xi) \\ 0 \end{pmatrix} + C_1 e^{|C_2|\xi}$ *for* $\xi < -\varepsilon^{-\frac{1}{4}}$;
- $\psi(\xi) = \begin{pmatrix} u_{\mathrm{R}}(0) \\ \hat{v}(\xi) \end{pmatrix} + O(\varepsilon^{\frac{3}{4}})$ *for* $\xi \in I_f$.

Here $u_{\mathrm{L/R}}$ are as given in (5.22)/(5.21) *and $\hat{v}$ as in* (5.10)*. The gauge constants $c_{\mathrm{L/R}}$ in* (5.22)/(5.21) *are determined by* (5.27)*.*

The connection with the original problem (5.5) is made in the following Corollary:

Corollary 5.6. *Assume that $(\mathcal{L} - \kappa)$ is invertible and that the functions A, B, C are even in each of their arguments. Then the function ψ as introduced in Lemma 5.5 is the unique, bounded solution to* (5.5)*.*

Proof. This proof is runs along the lines of the proof of Lemma 3.2. When the functions A, B, C are even in each of their arguments, both the operator $(\mathcal{L} - \kappa)$ –the left-hand side of (5.6)– and the right-hand side of (5.6) are symmetric in ξ. Therefore, $\psi(-\xi)$ must also solve (5.6). Since ψ is the unique solution to (5.6), it must be symmetric in ξ. The inner product $\langle \psi, \frac{\mathrm{d}}{\mathrm{d}\xi}\Gamma_h \rangle$ vanishes identically since $\frac{\mathrm{d}}{\mathrm{d}\xi}\Gamma_h$ is odd in ξ. We conclude that $\psi \in \mathcal{X}'$ and therefore ψ is the unique, bounded solution to (5.5). □

b) The parameter κ is zero. In this case, the homogeneous equation $\mathcal{L}\psi = 0$ has $\frac{\mathrm{d}}{\mathrm{d}\xi}\Gamma_h$ as bounded nontrivial solution. That means that any solution ψ to (5.6) is unique up to a multiple of $\frac{\mathrm{d}}{\mathrm{d}\xi}\Gamma_h$. We can use the projection Π_0 (3.11) to orthogonally decompose $\psi = C\,\frac{\mathrm{d}}{\mathrm{d}\xi}\Gamma_h + \psi_0$, where $C \in \mathbb{R}$ is free and $\langle \psi_0, \frac{\mathrm{d}}{\mathrm{d}\xi}\Gamma_h \rangle = 0$. The leading order analysis of the previous case a) can be directly applied to ψ, with $\hat{v}$ is substituted by v_0 (5.17). We can therefore state, analogous to Lemma 5.5:

Lemma 5.7. *Assume $\kappa = 0$, then the complete set of bounded solutions to* (5.6) *is given by the one-parameter family $(\psi_C)_{C\in\mathbb{R}}$, where $\psi_C = C\,\frac{\mathrm{d}}{\mathrm{d}\xi}\Gamma_h + \psi_0$ and $\Pi_0\psi_0 = 0$. For ψ_0, there are $C_{1,2} \in \mathbb{R}$ such that the following holds:*

- $\psi_0(\xi) = \begin{pmatrix} u_{\mathrm{R},0}(\varepsilon\xi) \\ 0 \end{pmatrix} + C_1 e^{-|C_2|\xi}$ *for* $\xi > \varepsilon^{-\frac{1}{4}}$;
- $\psi_0(\xi) = \begin{pmatrix} u_{\mathrm{L},0}(\varepsilon\xi) \\ 0 \end{pmatrix} + C_1 e^{|C_2|\xi}$ *for* $\xi < -\varepsilon^{-\frac{1}{4}}$;

- $\psi_0(\xi) = \begin{pmatrix} u_{\mathrm{R},0}(0) \\ v_0(\xi) \end{pmatrix} + O(\varepsilon^{\frac{3}{4}})$ *for* $\xi \in I_f$.

Here v_0 *is as in* (5.17)*, and*

$$u_{\mathrm{L/R},0}(x) = u_{\mathrm{L/R}}(x) - \frac{\int_{-\infty}^{0} u_{\mathrm{L}}(\hat{x}) \frac{\mathrm{d}U_h}{\mathrm{d}x}(\hat{x})\,\mathrm{d}\hat{x} + \int_{0}^{\infty} u_{\mathrm{R}}(\hat{x}) \frac{\mathrm{d}U_h}{\mathrm{d}x}(\hat{x})\,\mathrm{d}\hat{x}}{\int_{-\infty}^{\infty} \frac{\mathrm{d}U_h}{\mathrm{d}x}(\hat{x})^2\,\mathrm{d}\hat{x} + \int_{-\infty}^{\infty} \frac{\mathrm{d}V_h}{\mathrm{d}\xi}(\hat{\xi})^2\,\mathrm{d}\hat{\xi}} \frac{\mathrm{d}U_h}{\mathrm{d}x}(x) \tag{5.28}$$

with $u_{\mathrm{L/R}}$ *as in* (5.22)/(5.21)*. The gauge constants* $c_{\mathrm{L/R}}$ *in* (5.22)/(5.21) *are determined by* (5.27)*, with* $\hat{v}$ *replaced by* v_0*.*

Proof. For each C, the leading order expression for ψ_C is completely equivalent to that given in Lemma 5.5, with $\hat{v}$ replaced by v_0 (5.17) since $\kappa = 0$. Fixing C and adopting the notation of Lemma 5.5, the orthogonal projection of ψ_C onto the complement of the span of $\frac{\mathrm{d}}{\mathrm{d}\xi}\Gamma_h$ is to leading order given by

$$\frac{\int_{-\infty}^{0} u_L(\hat{x}) \frac{\mathrm{d}U_h}{\mathrm{d}x}(\hat{x})\,\mathrm{d}\hat{x} + \int_{0}^{\infty} u_R(\hat{x}) \frac{\mathrm{d}U_h}{\mathrm{d}x}(\hat{x})\,\mathrm{d}\hat{x} + \int_{-\infty}^{\infty} v_0(\hat{\xi}) \frac{\mathrm{d}V_h}{\mathrm{d}\xi}(\hat{\xi})\,\mathrm{d}\hat{\xi}}{\int_{-\infty}^{\infty} \frac{\mathrm{d}U_h}{\mathrm{d}x}(\hat{x})^2\,\mathrm{d}\hat{x} + \int_{-\infty}^{\infty} \frac{\mathrm{d}V_h}{\mathrm{d}\xi}(\hat{\xi})^2\,\mathrm{d}\hat{\xi}},$$

using Result 2.3 and (3.4). Since both v_0 and V_h are even functions of ξ, $\int_{-\infty}^{\infty} v_0(\hat{\xi}) \frac{\mathrm{d}V_h}{\mathrm{d}\xi}(\hat{\xi})\,\mathrm{d}\xi$ vanishes identically. □

The connection with the original problem (5.5) is made in the following Corollary:

Corollary 5.8. *Assume that* $\kappa = 0$ *and that the functions* A, B, C *are even in each of their arguments. Then the function* ψ_0 *as introduced in Lemma 5.7 is the unique, bounded solution to* (5.5)*. Moreover, we have* $u_{\mathrm{L/R},0} = u_{\mathrm{L/R}}$*.*

Proof. The first part of the proof, that $\psi_0 \in \mathcal{X}'$ and therefore ψ_0 is the unique, bounded solution to (5.5) for $\kappa = 0$, is completely analogous to the proof of Corollary 5.6. Moreover, since ψ_0 is even, we see that $u_{\mathrm{L}}(x) = u_{\mathrm{R}}(-x)$. As $\frac{\mathrm{d}}{\mathrm{d}\xi}\Gamma_h$ is odd and therefore $\frac{\mathrm{d}U_h}{\mathrm{d}x}(x) = -\frac{\mathrm{d}U_h}{\mathrm{d}x}(-x)$. Using these observations in (5.28) yields $u_{\mathrm{L/R},0} = u_{\mathrm{L/R}}$. □

Moreover, we can use the approach of section 5.2.1, case b) to easily obtain explicit expressions for the solutions $u_{\pm}$ to (5.20). The convergent function u_- is to leading order equal to the U-component of the translational eigenmode $\frac{\mathrm{d}}{\mathrm{d}\xi}\Gamma_h$, i.e.

$$u_-(x) = \frac{\mathrm{d}U_h}{\mathrm{d}x}(x) \quad \text{if} \quad \kappa = 0, \tag{5.29}$$

which in turn allows the divergent function u_+ to be expressed as

$$u_+(x) = u_-(x) \int_0^x \frac{1}{u_-(\hat{x})^2}\,\mathrm{d}\hat{x} \quad \text{if} \quad \kappa = 0. \tag{5.30}$$

Using integration by parts, this enables us to express $u_{\mathrm{L/R}}$ for $\kappa = 0$ more compactly as

$$u_{\mathrm{R}}(x) = u_-(x) \int_0^x \frac{1}{u_-(\hat{x})^2} \int_{\hat{x}}^{\infty} u_-(\tilde{x})\,[-A(\tilde{x})]\,\mathrm{d}\tilde{x}\,\mathrm{d}\hat{x} + c_{\mathrm{R}} u_-(x) \quad \text{if} \quad \kappa = 0, \tag{5.31a}$$

$$u_{\mathrm{L}}(x) = u_-(-x) \int_x^0 \frac{1}{u_-(-\hat{x})^2} \int_{-\infty}^{\hat{x}} u_-(-\tilde{x})\,[-A(\tilde{x})]\,\mathrm{d}\tilde{x}\,\mathrm{d}\hat{x} + c_{\mathrm{L}} u_-(-x) \quad \text{if} \quad \kappa = 0. \tag{5.31b}$$

5.3 Obtaining leading order expressions for a and b

We can use the results of section 5.2, as given in Lemmas 5.5 and 5.7 and their respective Corollaries 5.6 and 5.8 to obtain leading order expressions for the constituents of (4.12) and (4.13).

5.3.1 Leading order expression for Ψ_{20}

From section 4, we know that the coefficient Ψ_{20} is the unique solution to (4.8b). That equation is of the general form (5.5), with $\kappa = 2\,i\,\omega_H$ and

$$A(\varepsilon\xi) = -\nu_1 \frac{\mathrm{d}^2 F_1}{\mathrm{d}U^2}\,(\phi_H)_1^2\,, \tag{5.32a}$$

$$B(\varepsilon\xi, \xi) = -\nu_2 D^2 F_2(\phi_H, \phi_H), \tag{5.32b}$$

$$C(\varepsilon\xi, \xi) = -D^2 G(\phi_H, \phi_H). \tag{5.32c}$$

Since $(\mathcal{L} - 2\,i\,\omega_H)$ is invertible, Lemma 5.5 applies. Moreover, since all the partial derivatives of $F_{1,2}$ and G are evaluated at the components of the symmetric pulse $\Gamma_h = (U_h, V_h)^T$, we can use Corollary 5.6 to conclude that the leading order expression of Ψ_{20} can be found by applying Lemma 5.5 for the specific choices (5.32). Note that in this case, the solutions u_- to (5.20) and $\hat{v}$ as in (5.10) can be found by applying Result 2.4 for $\lambda = 2\,i\,\omega_H$.

5.3.2 Leading order expression for Ψ_{11}

Since $\mathcal{L}'$ is invertible on $\mathcal{X}'$, the coefficient Ψ_{11} is the unique solution to (4.8c). That equation is of the general form (5.5), with $\kappa = 0$ and

$$A(\varepsilon\xi) = -2\,\nu_1 \frac{\mathrm{d}^2 F_1}{\mathrm{d}U^2}\,\left|(\phi_H)_1\right|^2\,, \tag{5.33a}$$

$$B(\varepsilon\xi, \xi) = -2\,\nu_2 D^2 F_2(\phi_H, \overline{\phi_H}), \tag{5.33b}$$

$$C(\varepsilon\xi, \xi) = -2\,D^2 G(\phi_H, \overline{\phi_H}). \tag{5.33c}$$

Since $\kappa = 0$, Lemma 5.7 applies. Moreover, since all the partial derivatives of $F_{1,2}$ and G are evaluated at the components of the symmetric pulse $\Gamma_h = (U_h, V_h)^T$, we can use Corollary 5.8 to conclude that the leading order expression of Ψ_{11} can be found by applying Lemma 5.7 for the specific choices (5.33).

5.3.3 Leading order expression for $\Psi_{00}^{\hat{\mu}}$

Since $\mathcal{L}'$ is invertible on $\mathcal{X}'$, the coefficient $\Psi_{00}^{\hat{\mu}}$ is the unique solution to (4.8a). That equation is of the general form (5.5), with $\kappa = 0$ and

$$A(\varepsilon\xi) = -\nu_1 \frac{\mathrm{d}F_1}{\mathrm{d}U}\,\frac{\partial U_h}{\partial \mu}, \tag{5.34a}$$

$$B(\varepsilon\xi, \xi) = -\nu_2 \frac{\partial F_2}{\partial U}\,\frac{\partial U_h}{\partial \mu} - \nu_2 \frac{\partial F_2}{\partial V}\,\frac{\partial V_h}{\partial \mu}, \tag{5.34b}$$

$$C(\varepsilon\xi, \xi) = -\frac{\partial G}{\partial U}\,\frac{\partial U_h}{\partial \mu} - \frac{\partial G}{\partial V}\,\frac{\partial V_h}{\partial \mu}. \tag{5.34c}$$

Since $\kappa = 0$, Lemma 5.7 applies. Moreover, since all the partial derivatives of $F_{1,2}$ and G are evaluated at the components of the symmetric pulse $\Gamma_h = (U_h, V_h)^T$, we can use Corollary 5.8 to conclude that the leading order expression of $\Psi_{00}^{\hat{\mu}}$ can be found by applying Lemma 5.7 for the specific choices (5.34).

Moreover, we can use the general setting of section 5.2 to obtain a leading order expression for $\frac{\partial \Gamma_h}{\partial \mu}$ in terms of (...). By taking the partial derivative of the defining equation (2.2) for $(U, V) = (U_h, V_h)$, we see that $\frac{\partial \Gamma_h}{\partial \mu}$ obeys the linear equation

$$\mathcal{L}\frac{\partial \Gamma_h}{\partial \mu} = \begin{pmatrix} U_h \\ 0 \end{pmatrix}. \tag{5.35}$$

This equation is of the general form (5.6) with $\kappa = 0$, $B = 0$, $C = 0$ and $A(\varepsilon\xi) = U_h(\varepsilon\xi)$. We can therefore straightforwardly apply both Lemma 5.7 and Corollary 5.8 to obtain a leading order expression for $\frac{\partial\Gamma_h}{\partial\mu}$, ultimately in terms of Γ_h and $\frac{\mathrm{d}}{\mathrm{d}\xi}\Gamma_h$.

5.3.4 Using leading order expressions in the inner product

We now demonstrate how the specific choice of inner product (3.4) allows us to take advantage of the leading order expressions of the constituents of (4.12) and (4.13). We consider the inner product $\langle K, \overline{\phi_H^*}\rangle$ with

$$K(\varepsilon\xi,\xi) = \begin{pmatrix} A'(\varepsilon\xi) + \frac{1}{\varepsilon}B'(\varepsilon\xi,\xi) \\ C'(\varepsilon\xi,\xi) \end{pmatrix}, \tag{5.36}$$

where we assume that A', B', C' are exponentially decreasing as their arguments tend to $\pm\infty$, i.e.

$$\exists\, C^{A'}_{1,2,3,4} \in \mathbb{R} \quad : \quad \begin{cases} A'(x) \rightsquigarrow C_1^{A'}\, e^{-|C_2^{A'}|x} & \text{as} \quad x \to \infty \\ A'(x) \rightsquigarrow C_3^{A'}\, e^{|C_4^{A'}|x} & \text{as} \quad x \to -\infty \end{cases},$$

$$\exists\, C^{B'}_{1,2,3,4} \in \mathbb{R} \quad : \quad \begin{cases} B'(\varepsilon\xi,\xi) \rightsquigarrow C_1^{B'}\, e^{-|C_2^{B'}|\xi} & \text{as} \quad \xi \to \infty \\ B'(\varepsilon\xi,\xi) \rightsquigarrow C_3^{B'}\, e^{|C_4^{B'}|\xi} & \text{as} \quad \xi \to -\infty \end{cases},$$

and analogously for $C'(\varepsilon\xi,\xi)$. Using the definition of the inner product (3.4), we see that

$$\begin{aligned} \langle K, \overline{\phi_H^*}\rangle =& \varepsilon \int_{-\infty}^{\infty} A'(\varepsilon\xi)\, (\phi_H^*)_1\, \mathrm{d}\xi + \varepsilon \int_{-\infty}^{\infty} \frac{1}{\varepsilon} B'(\varepsilon\xi,\xi)\, (\phi_H^*)_1\, \mathrm{d}\xi + \int_{-\infty}^{\infty} C'(\varepsilon\xi,\xi)\, (\phi_H^*)_2\, \mathrm{d}\xi \\ =& \varepsilon \int_{-\infty}^{\infty} A'(\varepsilon\xi)\, u_{s,0}(\varepsilon\xi; i\,\omega_H)\mathrm{d}\xi + \int_{-\infty}^{\infty} B'(\varepsilon\xi,\xi)\, u_{s,0}(\varepsilon\xi; i\,\omega_H)\mathrm{d}\xi + \int_{-\infty}^{\infty} C'(\varepsilon\xi,\xi)\, v_{\mathrm{in}}^*(\xi; i\,\omega_H)\mathrm{d}\xi \\ =& \int_{-\infty}^{\infty} A'(x)\, u_{s,0}(x; i\,\omega_H)\, \mathrm{d}x + u_{s,0}(0; i\,\omega_H) \int_{-\infty}^{\infty} B'(0,\xi) + C'(0,\xi)\, v_{\mathrm{in}}^*(\xi; i\,\omega_H)\, \mathrm{d}\xi \end{aligned} \tag{5.37}$$

up to order $O\left(\varepsilon^{\frac{3}{4}}\right)$, using Lemma 5.1. Combining (4.5) with the resuls obtained in this section on the leading order behaviour of Ψ_{20}, Ψ_{11} and $\Psi_{00}^{\hat{\mu}}$, we see that every term in the inner products in (4.12) and (4.13) has the structure of $K(\varepsilon\xi,\xi)$ (5.36). Therefore, (5.37) can be straightforwardly applied to obtain explicit leading order expressions for a and b.

Based on the above analysis, we can make the following concluding observation:

Corollary 5.9. *Let $u_\pm(x)$ be the two linearly independent solutions to $(\mathcal{L}_s(x) - 2\,i\,\omega_H)\,u = 0$ for $x > 0$ (2.13) such that $u_\pm(x) \rightsquigarrow c_\pm e^{\pm\sqrt{\mu+2\,i\,\omega_H}\,x}$ as $x \to \infty$. Furthermore, let $v_{\mathrm{L/R}}(\xi)$ be the two linearly independent solutions to $\left(\mathcal{L}_f(\xi) - 2\,i\,\omega_H\right)v = 0$ for $\xi \in \mathbb{R}$ (2.12) such that $v_{\mathrm{L}}(\xi) \rightsquigarrow \hat{c}_{\mathrm{L}} e^{\sqrt{1+2\,i\,\omega_H}\,\xi}$ as $\xi \to -\infty$ and $v_{\mathrm{R}}(\xi) \rightsquigarrow \hat{c}_{\mathrm{R}} e^{-\sqrt{1+2\,i\,\omega_H}\,\xi}$ as $\xi \to \infty$.*
These functions, together with the leading order expression for ϕ_H as in Result 2.4 and the leading order expression for Γ_h as in Result 2.3 are sufficient to obtain the leading order expressions for the normal form coefficients a and b, as in (4.2).

6 Breathing pulses

The weakly nonlinear stability analysis given in sections 3 and 4 can now be used to investigate the dynamics of the pulse Γ_h (see Result 2.3) when it undergoes a destabilising Hopf bifurcation. The following is a version of Theorem 2.6 in [20].

Theorem 6.1 (**Existence and structure of breathing pulses**). *Let Γ_h be the pulse solution to* (2.2) *as established in Result 2.3. Assume that there exist parameter values $(\mu_H, \nu_{1,H}, \nu_{2,H})$ for which the spectrum of $\mathcal{L}$* (2.9) *is given by* (3.2). *Fix $\nu_1 = \nu_{1,H}$, $\nu_2 = \nu_{2,H}$ and let $\mu = \mu_H + \hat{\mu}$, with $0 < |\hat{\mu}| \ll 1$. Furthermore, take a and b as given in* (4.12) *resp.* (4.13).

- *If* $\operatorname{Re} b > 0$*, then the Hopf bifurcation is subcritical. For* $\hat{\mu} \operatorname{Re} a < 0$*, the pulse is stable; for* $\hat{\mu} \operatorname{Re} a > 0$ *, the pulse is unstable.*
- *If* $\operatorname{Re} b < 0$*, then the Hopf bifurcation is supercritical. For* $\hat{\mu} \operatorname{Re} a < 0$*, the pulse is stable; for* $\hat{\mu} \operatorname{Re} a > 0$ *, the pulse is linearly unstable. However, there exists a stable oscillating solution* $\Gamma_{\text{osc}}(\xi, t)$ *to* (2.2) *nearby, which is given by*

$$\Gamma_{osc}(\xi, t) = \Gamma_h(\xi) + \sqrt{|\hat{\mu}|} \sqrt{\left|\frac{\operatorname{Re} a}{\operatorname{Re} b}\right|} e^{i\,\omega_H\, t}\, \phi_H(\xi) + c.c. + O\left(|\hat{\mu}|\right). \tag{6.1}$$

Proof. The weakly nonlinear stability of Γ_h near a Hopf bifurcation is determined by the normal form equation (4.2). Writing $A(t) = r(t)\, e^{i\,\theta(t)}$, we obtain the system

$$\dot{r} = \hat{\mu} \operatorname{Re} a\, r + \operatorname{Re} b\, r^3 + O\left(r(|\hat{\mu}| + r^2)^2\right), \tag{6.2a}$$

$$\dot{\theta} = \omega_H + O\left(|\hat{\mu}| + r^2\right). \tag{6.2b}$$

The trivial equilibrium $r = 0$ of equation (6.2a) is stable when $\hat{\mu} \operatorname{Re} a < 0$ and unstable when $\hat{\mu} \operatorname{Re} a > 0$. Equation (6.2a) has a nontrivial leading order equilibrium if and only if there exists a positive solution $r = r_*$ to

$$r^2 = -\hat{\mu} \frac{\operatorname{Re} a}{\operatorname{Re} b}.$$

This equilibrium $r_* = O\left(\sqrt{|\hat{\mu}|}\right)$ has opposite stability to $r = 0$, i.e. r_* is stable if and only if $\hat{\mu} \operatorname{Re} a > 0$. Using (4.1) yields the expansion for $\Gamma_{\text{osc}}(\xi, t)$ (6.1). □

Numerical investigation of the normal form coefficients a (4.12) and b (4.13), by the explicit leading order analysis presented in section 5, can be combined with the result of Theorem 6.1 to obtain rigorous results on the existence and structure of breathing pulses in systems of the form (2.2).

6.1 Application: a slowly nonlinear Gierer-Meinhardt system

In [32], the existence and stability of pulse solutions as considered in section 2 was established for a slowly nonlinear Gierer-Meinhardt system, given by:

$$\begin{cases} U_t &= U_{xx} &- \left(\mu\, U - \nu_1 U^d\right) &+ \frac{\nu_2}{\varepsilon}\, V^2 \\ V_t &= \varepsilon^2 V_{xx} &- V &+ \frac{V^2}{U} \end{cases}. \tag{6.3}$$

The original Gierer-Meinhardt equation, a canonical model for morphogenesis which is studied extensively in the context of pattern formation [6, 9, 15, 21, 26, 28], can be recovered from (6.3) by setting $\nu_1 = 0$. The system (6.3) is of the form (2.1) with

$$F_1(U; \varepsilon) = U^d,\ d > 1, \quad F_2(U, V; \varepsilon) = V^2, \quad G(U, V; \varepsilon) = \frac{V^2}{U}. \tag{6.4}$$

The nonlinearities F_2 and G are chosen according to the 'classical' Gierer-Meinhardt model. The 'slow' nonlinearity F_1 is absent in the Gierer-Meinhardt model, but was introduced in [32] to study the influence of such a slow nonlinearity on the pulse construction and stability.
It can easily be verified that the above choice for $F_{1,2}$ and G (6.4) satisfies Assumptions 2.2 (A1 - A4). The reduced fast system (2.5) takes the form $v_{f,\xi\xi} = v_f - \frac{1}{u_0} v_f^2$, which has a homoclinic solution

$$v_{f,h}(\xi; u_0) = \frac{3u_0}{2} \operatorname{sech}^2 \frac{1}{2} \xi, \tag{6.5}$$

satisfying Assumptions 2.2, (A5). Using this homoclinic solution, $D_p(u_0)$ (2.7) can be calculated as

$$D_p(u_0) = \int_{\infty}^{\infty} \left(v_{f,h}(\xi; u_0)\right)^2 \mathrm{d}\xi = 6u_0^2, \tag{6.6}$$

which means that Assumptions 2.2, (A6) is satisfied once the factor 6 is scaled out by rescaling $\nu_2 \to \hat{\nu}_2 = 6\nu_2$. The choice of F_1 realises the reduced slow system (2.6) as $u_{s,xx} = \mu\, u_s - \nu_1 u_s^d$, which also has an orbit homoclinic to the origin. The u-component of this orbit, which is in particular forward asymptotic to the origin, is given by the function

$$u_{s,0}(x) = \left(\frac{\mu(d+1)}{2\nu_1}\,\mathrm{sech}^2\,\frac{1}{2}(d-1)\,\sqrt{\mu}\,x\right)^{\frac{1}{d-1}}. \tag{6.7}$$

The pulse existence condition (2.8) becomes

$$\frac{2\nu_1}{d+1}u^{d-1} = \mu - \frac{3}{2}\hat{\nu}_2 u^2, \tag{6.8}$$

which always has precisely one positive solution $u = u_*$. Using the above, Result 2.3 yields the existence and leading order expression of the pulse solution to (6.3), which we will denote by Γ_h^{nGM}.
The fast linear operator (2.12) takes the form

$$\mathcal{L}_f(\xi) = \frac{\mathrm{d}^2}{\mathrm{d}\xi^2} - \left[1 - 3\,\mathrm{sech}^2\,\frac{1}{2}\xi\right], \quad \xi \in \mathbb{R}, \tag{6.9}$$

which has eigenvalues $\lambda_{f,0} = \frac{5}{4}$, $\lambda_{f,1} = 0$ and $\lambda_{f,2} = -\frac{3}{4}$. The slow linear operator (2.13) is realised as

$$\mathcal{L}_s(x) = \frac{\mathrm{d}^2}{\mathrm{d}x^2} - \mu\left[1 - \frac{d(d+1)}{2}\,\mathrm{sech}^2\,\frac{1}{2}(d-1)\,\sqrt{\mu}\,(x_* + x)\right], \quad x \geq 0. \tag{6.10}$$

Both equations can be solved explicitly in terms of associated Legendre functions [3], see [32] for a full and detailed analysis.

As in the general case [11], the eigenvalues for the pulse solution Γ_h^{nGM} to (6.3) can be determined using Evans function techniques. In [32], an explicit leading order expression for the Evans function was found in terms of associated Legendre functions, see Theorem 3.10 in [32]. This leading order Evans function can be directly numerically evaluated for different parameter values. In Figure 4, the pulse eigenvalues are plotted in the complex plane for fixed $\nu_{1,2}$ and d, while varying μ. Here, the influence of the slow nonlinear term $F_1(U) = U^d$ (6.4) can be clearly seen. For $d = 2$, the eigenvalue orbit crosses the imaginary axis for $\mu = \mu_H = 1.47986\ldots$ at $\lambda = i\,\omega_H = 1.47638\ldots i$, and it becomes clear that the pulse is stable for all $\mu > \mu_H$ (see [32], Theorem 4.6). However, for $d = 5$, the eigenvalue orbit exhibits a different behaviour. After an initial stabilising Hopf bifurcation for $\mu = \mu_{H,1} = 0.4173\ldots$ at $\lambda = i\,\omega_{H,1} = 0.958684\ldots i$, the eigenvalue orbit turns around and undergoes a second, destabilising Hopf bifurcation for $\mu = \mu_{H,2} = 5.134\ldots$ at $\lambda = i\,\omega_{H,1} = 3.78646\ldots i$.

This turning behaviour is general for $d > 3$, see [32], Theorem 4.7. That means that for all $d > 1$, there is an neighbourhood of $(\nu_1, \nu_2) = (2, \frac{1}{2})$ in parameter space such that there is a (possibly bounded) interval in μ for which the pulse Γ_h^{nGM} is stable. At the boundary of this interval, the pulse destabilises through a Hopf bifurcation. Since our parameter space $\{(\mu, \nu_1, \nu_2, d)\}$ is four-dimensional, we can determine the (boundaries of the) stability region by intersecting it with two-dimensional hyperplanes, i.e. by fixing two parameters. In Figure 5, the boundary of this stability region is determined for different values of d and ν_1, with μ and ν_2 as free parameters. The two Hopf bifurcation values for $d = 5$, $\nu_1 = 2$, $\nu_2 = \frac{1}{2}$ are indicated on the blue

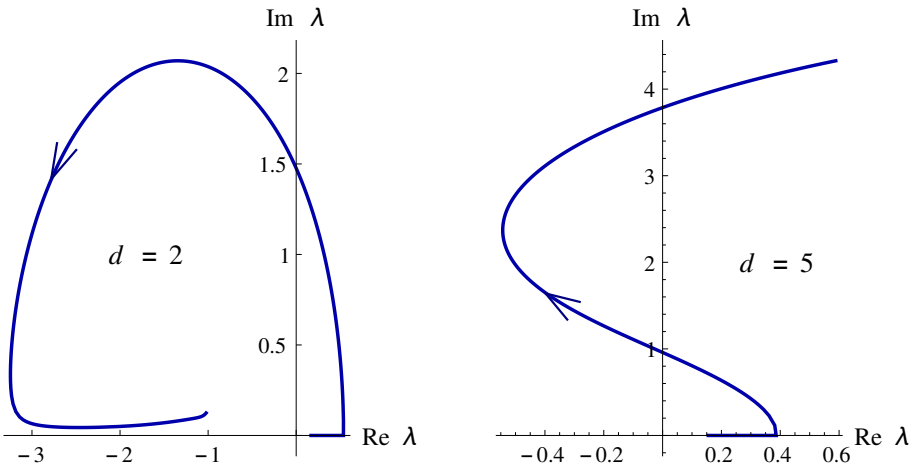

Figure 4: The eigenvalues of the pulse solution to (6.3) to leading order in ε as a function of increasing μ, indicated by the arrow. Since the pulse eigenvalues come in complex conjugated pairs, only the upper half of the complex plane is shown. Here, $\nu_1 = 2$ and $\nu_2 = \frac{1}{2}$ (i.e. $\hat{\nu_2} = 3$) are fixed. For $d = 2$ (left figure), the pulse undergoes one stabilising Hopf bifurcation for $\mu = \mu_H = 1.47986\ldots$ at $\lambda = i\,\omega_H = 1.47638\ldots i$. For $d = 5$ (right figure), a second, destabilising Hopf bifurcation takes place for $\mu = \mu_{H,2} = 5.134\ldots$ at $\lambda = i\,\omega_{H,1} = 3.78646\ldots i$, while the first Hopf bifurcation is at $\mu = \mu_{H,1} = 0.4173\ldots$ with $\lambda = i\,\omega_{H,1} = 0.958684\ldots i$ for these parameter values.

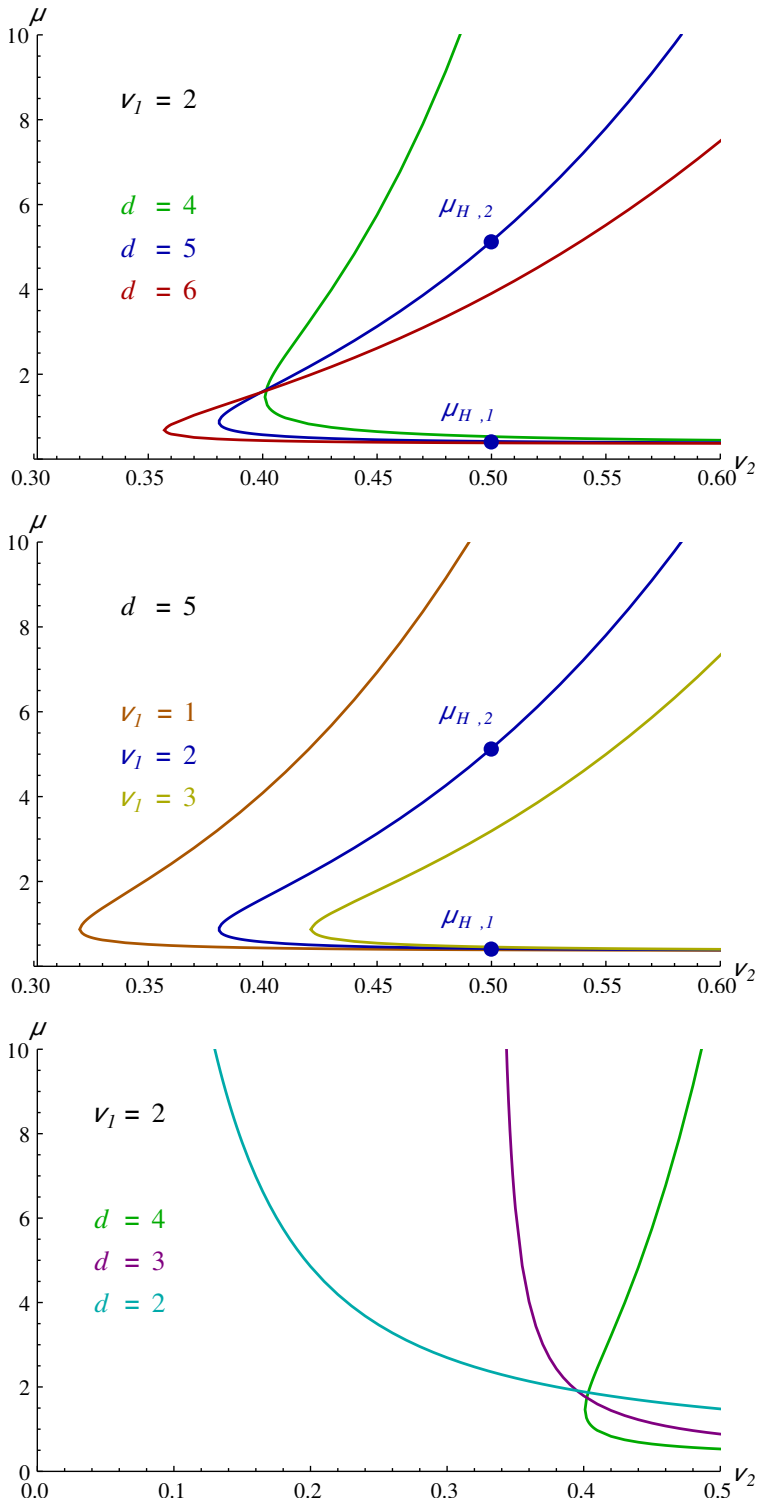

Figure 5: Curves of Hopf bifurcation parameter values in the (ν_2, μ)-plane. Top, $\nu_1 = 2$; bifurcation curves are plotted for $d = 4, 5, 6$. Middle, $d = 5$; bifurcation curves are plotted for $\nu_1 = 1, 2, 3$. Bottom, $\nu_1 = 2$, bifurcation curves are plotted for $d = 2, 3, 4$. These curves form the boundary of the region in parameter space for which the pulse Γ_h^{nGM} is stable. In the top and middle figures, the bifurcation values $\mu_{H,1} = 0.4173\ldots$ and $\mu_{H,2} = 5.134\ldots$ for $d = 5, \nu_2 = \frac{1}{2}$ are indicated, c.f. Figure 4 (right).

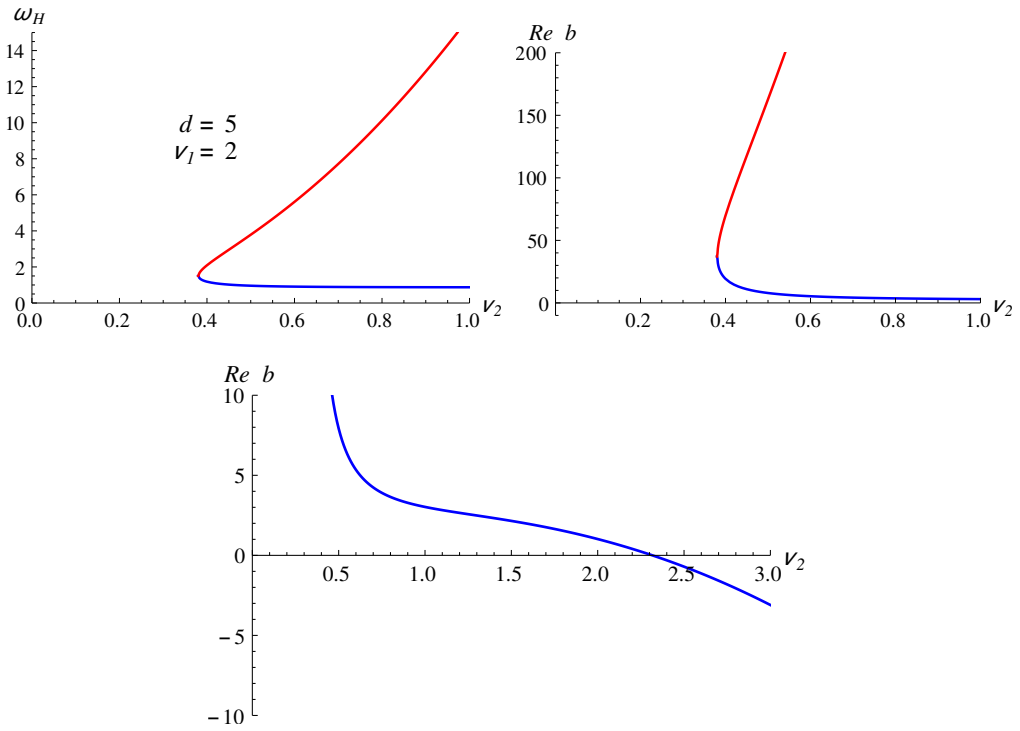

Figure 6: In the left figure, the Hopf frequencies are plotted as a function of ν_2, for $d = 5$ and $\nu_1 = 2$. The lower branch, representing $\omega_{H,1}$, is indicated in blue; the upper branch, representing $\omega_{H,2}$, is indicated in red. In the right figure, the value of Re b is plotted, using corresponding colors. It can be seen that the the value of Re b corresponding to $\omega_{H,1}$ changes sign at $\nu_2 = \nu_2^* = 2.3196\ldots$; there, the nature of this lower branch Hopf bifurcation changes from subcritical to supercritical.

curve in both figures. The Hopf bifurcations merge into a singular Hopf bifurcation where the bifurcation curves meet in a fold.

In Figure 6, left, the Hopf frequencies for $d = 5$ and $\nu_1 = 2$ are plotted as a function of the parameter ν_2. The merging of Hopf bifurcations can again be observed. For these Hopf eigenvalues, the normal form coefficient b (4.13) was calculated according to Corollary 5.9. It can be seen that the Hopf bifurcations of the upper branch have a positive –even large– value of Re b, and are therefore subcritical (Theorem 6.1). However, for the lower branch of Hopf bifurcations, it is seen that the sign of Re b can change. Note that this lower branch corresponds with the stabilising Hopf bifurcation $\lambda = i\,\omega_{H,1}$ which is present for all d, see Figure 4. A collection of such curves of Re b is shown in Figure 7, based on the associated Hopf curves from Figure 5. It is clear that this crossing from sub- to supercriticality is a general phenomenon, and is therefore not restricted to the specific choice of parameters used to produce these Figures.

The direct numerical evaluation of Re b, made possible by the result of Corollary 5.9, enables us to draw conclusions about the sub- or supercriticality of the Hopf bifurcations of pulses in the slowly nonlinear Gierer-Meinhard model (6.3). Based on the criticality curves shown in Figure 7, we can take a well-chosen point in parameter space, e.g. $(\nu_1, \nu_2, d) = (2, 3, 5)$, such that one of the two Hopf bifurcations for this parameter triplet is subcritical, and the other supercritical. By continuous dependence on parameters, we can then state the following Theorem:

Theorem 6.2. *Let $\varepsilon > 0$ be sufficiently small. There exists an open nonempty neighbourhood*

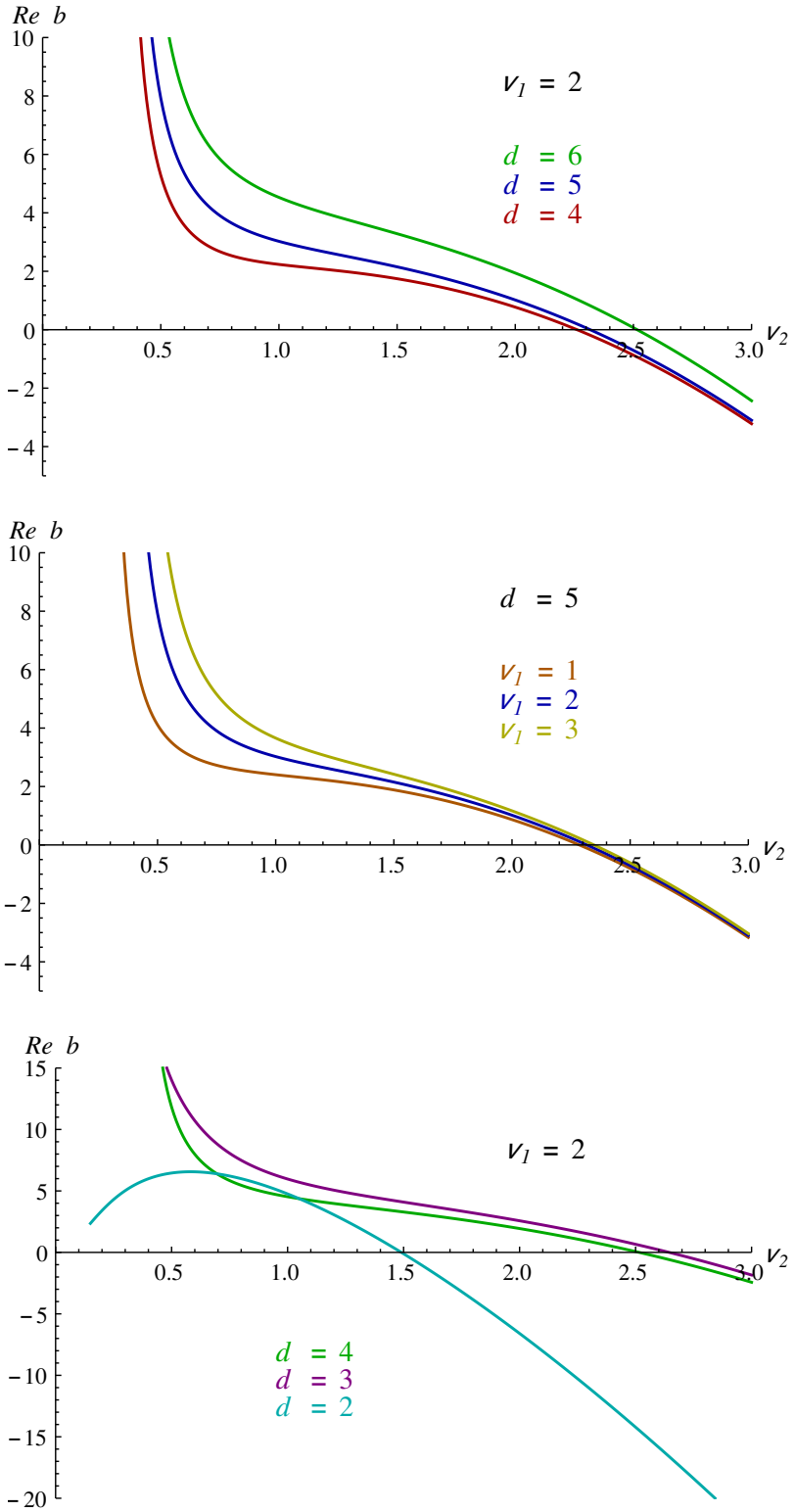

Figure 7: An overview of several criticality curves, corresponding to the Hopf bifurcation curves shown in Figure 5. The color coding coincides. It can be seen that the transition from sub- to supercriticality is a general phenomenon for pulse solutions of (6.3).

$\mathcal{V}$ in (ν_1, ν_2, d)-parameter space such that the following holds. For any $(\nu_1, \nu_2, d) \in \mathcal{V}$, there are two Hopf bifurcation values $\mu_{H,1}(\nu_1, \nu_2, d)$ and $\mu_{H,2}(\nu_1, \nu_2, d)$ with $\mu_{H,1} < \mu_{H,2}$ for which the associated pulse eigenvalues are given by $\lambda_{H,1} = i\,\omega_{H,1}$ resp. $\lambda_{H,2} = i\,\omega_{H,2}$ with $\omega_{H,1}, \omega_{H,2} \in \mathbb{R}$. The Hopf bifurcation $\lambda_{H,1} = i\,\omega_{H,1}$ is supercritical; the Hopf bifurcation $\lambda_{H,2} = i\,\omega_{H,2}$ is subcritical.

In Figure 8, the leading order results of the theory presented in this paper are compared with direct numerical simulations using the `pdepe` routine in MATLAB [1], for $\varepsilon = 0.01$. The results of the analysis, which predicts a supercritical Hopf bifurcation and therefore by Theorem 6.1 a stable breathing pulse, are reflected in the numerical simulations, where such a breathing pulse is indeed observed.

It is now quite straightforward to obtain a result which was suggested, but not confirmed, in previous literature on the 'canonical' Gierer-Meinhardt system, i.e. (6.3) with $\nu_1 = 0$. In [6], the existence and stability of pulse solutions in Gierer-Meinhardt type systems was established using ideas similar to those used in [32] and [11]. There, it was shown that for $\mu = \mu_H = 0.36\ldots$, the pulse undergoes a Hopf bifurcation. Numerical simulations [8, 34] suggested that this Hopf bifurcation is subcritical. This observation is confirmed by direct numerical evaluation of (the real part of) the normal form coefficient b, which has the value $\operatorname{Re} b = 0.48\ldots > 0$. As a consequence, the following Corollary is a direct result from numerical evaluations equivalent to those underlying Theorem 6.2:

Corollary 6.3. *Let $\varepsilon > 0$ be sufficiently small. The Hopf bifurcation associated to the classical Gierer-Meinhardt pulse is subcritical.*

7 Discussion

The research presented in this paper was inspired by the observation of stable oscillating pulses in the slowly nonlinear Gierer-Meinhardt model, see [32], section 5. There, it was shown that numerical simulations of the full PDE system suggested the existence of breathing pulses (possibly with a dynamically modulated amplitude) near parameter values for which the stationary pulse undergoes a Hopf bifurcation. The hypothesis that such a Hopf bifurcation could be the 'birthplace' of these breathing pulses is confirmed in the current paper. A consequence of the supercriticality of the Hopf bifurcation, established in Theorem 6.2, is that stable periodically modulated pulse amplitudes (i.e. breathing pulses) can and do indeed exist.

However, this is not the end of the story. The centre manifold associated to the Hopf bifurcation has only been expanded up to third order. A fifth order expansion, for example near the generalised Bautin point where the Hopf bifurcation transgresses from sub- to supercriticality, can in principle be carried out. This would entail performing an analysis analogous to that presented in sections 4 and 5, using the extended fifth order normal form

$$\frac{\mathrm{d}A}{\mathrm{d}t} = i\,\omega_H\,A + \left(a_0\,\hat{\mu} + a_1\,\hat{\mu}^2\right)A + (b_0 + b_1\,\hat{\mu})\,A\,|A|^2 + c\,A\,|A|^4 + O\left(A(|\hat{\mu}| + |A|^2)^3\right), \qquad (7.1)$$

compare (4.2). This way, the first steps towards a more encompassing description of the dynamically modulated pulse amplitude near Hopf bifurcations can be taken. Numerical results from [32], section 5 suggest that this amplitude can be quasiperiodically or even chaotically modulated. Note that (7.1) allows for a $\hat{\mu}$-independent periodic orbit with radius $\sqrt{-\frac{b_0}{c}}$, which might interact with the stable pulse near a Hopf bifurcation for sufficiently large perturbations.

It is worthwhile to note that the procedure to obtain explicit expressions for the Hopf normal form, as presented in this paper, is not restricted to the stationary pulse solution, which

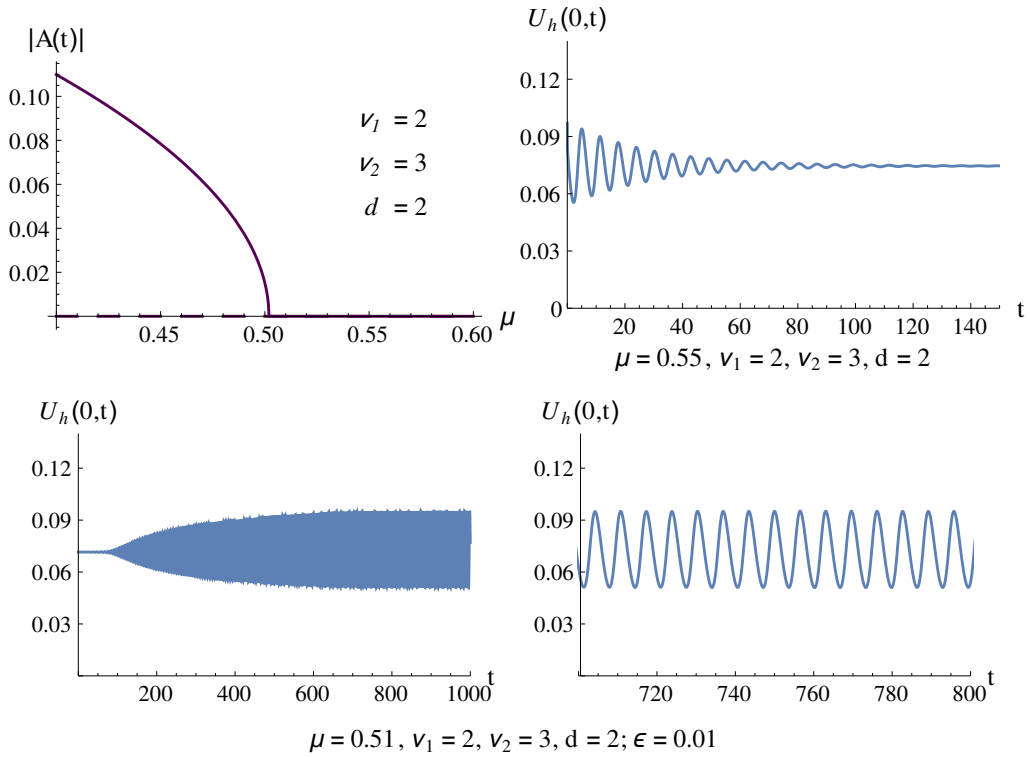

Figure 8: Top left, the pulse amplitude modulation $|A(t)|$ (4.1) is plotted as a function of the principal bifurcation parameter μ, for $(\nu_1, \nu_2, d) = (2, 3, 2)$. As μ decreases, a stable oscillating pulse bifurcates at $\mu = \mu_{H,1} = 0.502\ldots$; the now unstable stationary pulse is indicated by the dashed line. The other figures show the results of a direct numerical simulation of the full system (2.1), presented by a plot of the U-component of the pulse tip at $x = 0$ as a function of time. The simulations were obtained by the `pdepe` routine in MATLAB [1], for the parameter values $(\nu_1, \nu_2, d) = (2, 3, 2)$ and $\varepsilon = 0.01$. Top right, for $\mu = 0.55$, the pulse is seen to be stable under perturbations. As μ is decreased to $\mu = 0.51$, we see a small perturbation leading to a stable oscillating pulse (bottom left). The oscillation of the pulse tip can be observed more clearly in a segment of the simulated time domain (bottom right). We see that the results of the direct numerical simulations argree very well with the leading order analysis.

was analysed in [32] and [11]. The procedure is in principle valid for (multi)pulses and fronts in singularly perturbed reaction-diffusion systems: as long as one is able to obtain an explicit expression for the stationary pattern (and, more importantly, for its eigenfunctions), the techniques presented in this paper can be used to obtain an explicit expression for the normal form expansion coefficients, which can be directly numerically evaluated, allowing one to gain more insight in the dynamical properties of the pattern under consideration.

Acknowledgement The author would like to thank Arjen Doelman, Jens Rademacher and especially Hermen Jan Hupkes for the helpful discussions and useful suggestions during the writing of this paper.

References

[1] The MathWorks, Inc., MATLAB Release 2014b.

[2] Wolfram Research, Inc., Mathematica, Version 9.0, 2012.

[3] NIST Digital Library of Mathematical Functions: Legendre and Related Functions. `http://dlmf.nist.gov/14`, 2014.

[4] P.C. Bressloff, S.E. Folias, A. Prat, and Y-X. Li. Oscillatory waves in inhomogeneous neural media. *Physical Review Letters*, 91(17):178101, 2003.

[5] W. Chen and M.J. Ward. Oscillatory instabilities of multi-spike patterns for the one-dimensional Gray-Scott model. *European Journal of Applied Mathematics*, 20(2):187 – 214, 2009.

[6] A. Doelman, R.A. Gardner, and T.J. Kaper. Large Stable Pulse Solutions in Reaction-diffusion Equations. *Indiana University Mathematics Journal*, 50:443 – 507, 2001.

[7] A. Doelman, R.A. Gardner, and T.J. Kaper. *A stability index analysis of 1-D patterns of the Gray-Scott model*, volume 155 of *Memoirs of the Americal Mathematical Society*. American Mathematical Society, 2002.

[8] A. Doelman, T.J. Kaper, and R.A. Gardner. Stability analysis of singular patterns in the 1D Gray-Scott model: a matched asymptotics approach. *Physica D: Nonlinear Phenomena*, 122:1–36, 1998.

[9] A. Doelman, T.J. Kaper, and K. Promislow. Nonlinear asymptotic stability of the semi-strong pulse dynamics in a regularized Gierer-Meinhardt model. *SIAM Journal on Mathematical Analysis*, 38(6):1760 – 1787, 2007.

[10] A. Doelman, J. Rademacher, and S. van der Stelt. Hopf dances near the tips of busse balloons. *Discrete and Continuous Dynamical Systems*, 5:61–92, 2012.

[11] A. Doelman and F. Veerman. An explicit theory for pulses in two component, singularly perturbed, reaction-diffusion equations. *Journal of Dynamics and Differential Equations*, 2013.

[12] W.J. Firth, G.K. Harkness, A. Lord, J.M. McSloy, D. Gomila, and P. Colet. Dynamical properties of two-dimensional kerr cavity solitons. *Journal of the Optical Society of America B: Optical Physics*, 19(4):747–752, 2002.

[13] S.E. Folias. Nonlinear analysis of breathing pulses in a synaptically coupled neural network. *SIAM Journal on Applied Dynamical Systems*, 10(2):744–787, 2011.

[14] S.E. Folias and P.C. Bressloff. Breathing pulses in an excitatory neural network. *SIAM Journal on Applied Dynamical Systems*, 3(3):378–407, 2004.

[15] A. Gierer and H. Meinhardt. A theory of biological pattern formation. *Kybernetik*, 12:30–39, 1972.

[16] D. Gomila, P. Colet, M.A. Matías, G-L. Oppo, and M. San Miguel. Localized structures in nonlinear optical cavities. In A.M. Sergeev, editor, *Topical Problems of Nonlinear Wave Physics*, volume 5975 of *Proceedings of SPIE*, page 59750U. S.P.I.E., 2006.

[17] P. Gray and S.K. Scott. Autocatalytic reactions in the isothermal, continuous stirred tank reactor: isolas and other forms of multistability. *Chemical Engineering Science*, 38:29–43, 1983.

[18] S.V. Gurevich, S. Amiranashvili, and H-G. Purwins. Breathing dissipative solitons in three-component reaction-diffusion system. *Pysical Review E: Statistical, Nonlinear, and Soft Matter Physics*, 74:066201, 2006.

[19] S.V. Gurevich and R Friedrich. Moving and breathing localised structures in reaction-diffusion systems. *Mathematical Modelling of Natural Phenomena*, 8(5):84–94, 2013.

[20] M. Haragus and G. Iooss. *Local Bifurcations, Center Manifolds, and Normal Forms in Infinite-Dimensional Dynamical Systems*. Springer, 2011.

[21] D. Iron, M.J. Ward, and J. Wei. The stability of spike solutions to the one-dimensional Gierer-Meinhardt model. *Physica D: Nonlinear Phenomena*, 150:25 – 62, 2001.

[22] T. Kolokolnikov, M.J. Ward, and J. Wei. The existence and stability of spike equilibria in the one-dimensional Gray-Scott model: the low feed rate regime. *Studies in Applied Mathematics*, 115(1):21 – 71, 2005.

[23] B. Sandstede and A. Scheel. Essential instabilities of fronts: bifurcation, and bifurcation failure. *Dynamical Systems*, 16(1):1–28, 2001.

[24] B. Sandstede, A. Scheel, and C. Wulff. Dynamics of spiral waves on unbounded domains using center-manifold reductions. *Journal of Differential Equations*, 141:122–149, 1997.

[25] W. Sun, M.J. Ward, and R. Russell. The slow dynamics of two-spike solutions for the Gray-Scott and Gierer-Meinhardt systems: competition and oscillatory instabilities. *SIAM Journal on Applied Dynamical Systems*, 4(4):904 – 953, 2005.

[26] I. Takagi. Point-condensation for a reaction-diffusion system. *Journal of Differential Equations*, 61:208 – 249, 1986.

[27] D. Turaev, A.G. Vladimirov, and S. Zelik. Long-range interaction and synchronization of oscillating dissipative solitons. *Physical Review Letters*, 108:263906, 2012.

[28] H. van der Ploeg and A. Doelman. Stability of spatially periodic pulse patterns in a class of singularly perturbed reaction-diffusion equations. *Indiana University Mathematics Journal*, 54(5):1219 – 1301, 2005.

[29] S. van der Stelt, A. Doelman, G.M. Hek, and J. Rademacher. Rise and fall of periodic patterns for a generalized Klausmeier-Gray-Scott model. *Journal of Nonlinear Science*, 23(1):39 – 95, 2013.

[30] P. van Heijster, A. Doelman, and T.J. Kaper. Pulse dynamics in a three-component system: Stability and bifurcations. *Physica D: Nonlinear Phenomena*, 237:3335–3368, 2008.

[31] P. van Heijster, A. Doelman, and T.J. Kaper. Pulse dynamics in a three-component system: Existence analysis. *Journal of Dynamics and Differential Equations*, 21:73–115, 2009.

[32] F. Veerman and A. Doelman. Pulses in a Gierer-Meinhardt equation with a slow nonlinearity. *SIAM Journal on Applied Dynamical Systems*, 12(1):28–60, 2013.

[33] A.G. Vladimirov, S.V. Fedorov, N.A. Kaliteevskii, G.V. Khodova, and N.N. Rosanov. Numerical investigation of laser localized structures. *Journal of Optics B: Quantum and Semiclassical Optics*, 1(1):101–106, 1999.

[34] M.J. Ward and J. Wei. Hopf bifurcation and oscillatory instabilities of spike solutions for the one-dimensional Gierer-Meinhardt model. *Journal of Nonlinear Science*, 13:209–264, 2003.